MARSHALL GRANT

IN-76-CR 118030 p.64

FINAL REPORT

TITLE OF GRANT
Further Improvements in Program to Calculate Electronic Properties of Narrow Band Gap Materials

TYPE OF REPORT
Brief Summary of Entire Project

NAME OF PRINCIPAL INVESTIGATOR
James D. Patterson
September 15, 1992

PERIOD COVERED BY THE REPORT
June 15, 1991 - June 15, 1992
(plus extension of up to six months)

NAME AND ADDRESS OF GRANTEE INSTITUTION
Florida Institute of Technology
150 W. University Boulevard
Melbourne, FL 32901

GRANT NUMBER
NAG8-781 Supplement 2
George C. Marshall Space Flight Center
Marshall Space Flight Center, AL 35812
(Technical Officer Sandor L. Lehoczky, ES75)

Personnel

James D. Patterson, Principal Investigator
Professor and Head, Physics and Space Sciences Department
Florida Institute of Technology

Wafaa Abdelhakiem Gobba, Post Doctoral Research Associate
Physics and Space Sciences Department
Florida Institute of Technology

ABSTRACT

We list and discuss the tasks we have accomplished and considered. In some areas more has been accomplished than others. An extra task was a calculation comparing electron mobilities in Mercury Manganese Telluride with Mercury Cadmium Telluride given in 1H. We then list the reports and papers produced and follow that with either abstracts or the papers themselves. In one key paper we obtain good results between experiment and theory in Mercury Zinc Telluride and also find it typically has mobilities competitive with Mercury Cadmium Telluride. In the appendix we have a relatively complete set of references.

Outline

I. LIST OF TASKS ACCOMPLISHED/CONSIDERED

A. Characterization of Donors and Acceptors

The study of donors and acceptors in narrow gap semiconductors is by no means simple. Misplaced Hg in MCT seems to be a major cause of intrinsic doping. Hg vacancies can produce a p type material and extra Hg interstitials an n type. Indium doping has caused p type MCT to become n type as expected. A little more generally, group I and II elements should be acceptors and donors on Hg, Cd (group II) metal sites while V and VII elements should be acceptors and donors on Te (group VI) sites. The situation is very complicated, however, and experiment is needed to verify these suppositions. Furthermore, the situation is complicated by the fact that we can have both deep and shallow states. Vacancies, interstitials and even substitutional impurities can cause deep levels. In any case deep levels produced by a short range potential, are often not well characterized, and usually produce a level near the middle of the gap. If we neglect deep levels, we are still left with shallow levels. Shallow states can, at least for small x, merge with the conduction band. We can understand this merger as related to the Mott transition. When the density of defects increases, discrete levels may become broadened and produce energy states that may join with, for example, the conduction band in the case of donors. In fact, it has been predicted that $Hg_{1-x}Cd_xTe$ with a (shallow) donor concentration of at least 10^{14} cm^{-3} would not have bound states and this seems to be well confirmed experimentally. In general there appears to be no freezeout of carriers on shallow impurities for bandgaps in, as grown, MCT which has $x < .2$. There are in fact other reasons for the merging with the conduction band. Donor levels can be screened by electrons in the conduction band and this screening can decrease the binding energy. We have examined this in a paper referenced below. In addition, when the binding energy gets small enough the donor wave functions may hybridize with the band functions and again we get merging.

Note about shallow donors.

The simplest theory of shallow impurities characterizes them as hydrogenic. For non-degenerate bands with parabolic dispersion relations, the "envelope" function of the impurities satisfies;

$$\left[- \frac{\hbar^2}{2m^*} \nabla^2 - \frac{e^2}{Kr} \right] F = E F$$

where m^* is the effective mass and K is the (relative) dielectric constant.

For a 1s ground state , the binding energy is $$E_B = \frac{13{,}600}{K^2}\,\frac{m^*}{m_o} \quad \text{mev}$$

with wave function

$$F_{1s} = \frac{1}{\sqrt{\pi\, a_B^3}}\; e^{r/a_B}$$

where

$$a_B = 0.53 \times K \times \frac{m_o}{m^*}\,\text{Å}$$

Our situation has many complications beyond this (Bastard p. 119-120). We don't have parabolic bands and the donors are often not well characterized. Another complication arises from the fact that in the compound semiconductors that we consider, the lattice is charged so electrons interact with it even at absolute zero. Thus the stationary states are polarons. The effect of the lattice can only be neglected for tightly bound electrons - not the usual case for shallow donors. For weak binding one must view the situation as a polaron bound in a hydrogenic orbit

SUMMARY - SHALLOW LEVEL DEFECTS

These have a long range potential and their wave function spreads over many neighboring atoms.

Have a hydrogen like spectrum as modified by dielectric constant and effective mass.

Usually have ionization energies much less than the gap energy.

Connected to the adjacent band (that is Eigenfunction mix with nearest band states).

Due to screening and hybridization may merge with nearest band.

They control conductivity.

Note about deeper levels.

The nature of donors in $Ga_{1-x}Al_xAs$ can be quite different depending on the x value (Weisbuch and Vinter, 47-50). For Si donors the energy levels can change from 6 meV to 160 meV as one changes from direct to indirect materials. The transition takes place at about x = 0.24.

Erbarut has treated the electronic structure of ideal vacancies in MCT. His work is based on an extension of the Slater-Koster model and does not include lattice relaxation. The energy levels obtained are often in the range of deep bound levels. At any rate, deep levels are often treated along Slater-Koster lines. Effective mass techniques are often not appropriate for deep levels. Hjalmarson has defined a deep impurity to be one "whose short-range central-cell potential alone is sufficiently strong to bind a state".

SUMMARY - DEEP LEVEL DEFECTS

Short range potential, wave function relatively well localized.

Not a hydrogen like spectrum - use tight binding approximation.

Often have ionization energy comparable to half the gap energy.

Connected to the conduction band and valence band.

Often hard to even identify a model for center.

They control lifetime of carriers.

General note.

Capper has given a review of impurity behavior in bulk MCT. He points out that "extensive doping using elements which provide stability of electrical properties will become increasingly important in future infrared devices based on MCT." A common way to study defects is by photoluminescence spectra as discovered by Werner et al. Native defects are highly sensitive to deviations in stochiometry and to stress. Point defects come in a variety of forms; lattice defects (vacancy, self interstitial and antisite) and foreign atom (substitutional and interstitial).

Donors, acceptors and other defects can be important in lowering the mobility at low temperature, but other scattering mechanisms are much more important at higher temperatures. Defects determine to a large extent the quality of these materials for infrared detectors.

REFERENCES

1. J.D. Patterson and Wafaa A. Gobba, "Enhanced Screening in Doped Semiconductors," Bull. Am. Phys. Soc. 37 (1), 196 (1992).

2. E. Erbarut, "Electronic Structure of the Ideal Vacancies in (Hg, Cd) Te," phys. stat. sol. (b) 164, 235-241 (1991).

3. P. Capper, "A Review of Impurity Behavior in Bulk and Epitaxial $Hg_{1-x}Cd_xTe$," J. Vac. Sci. Technol. B9(3), 1667-1681 (1991).

4. L. Werner, J.W. Tomm and K.H. Herrmann, "Identification of the Nature of the Optical Transitions in $Hg_{0.42}Cd_{0.58}Te$," Infrared Phys. 31(1), 49-58 (1991).

5. M.A. Berding, M. van Schilfgaarde, A.T. Paxton, and A. Sher, "Defects in ZnTe, CdTe, and HgTe: Total Energy Calculations," J. Vac. Sci. Technol. A 8(2) 1103-1107 (1990).

6. C.L. Littler, D.G. Seiler, and M.R. Loloee, "Magneto-optical Investigation of Impurity and Defect Levels in HgCdTe Alloys," J. Vac. Sci. Technol. A 8(2), 1133-1138 (1990).

7. J.B. Choi and H.D. Drew, "Donor Spectroscopy in $Hg_{1-x}Cd_xTe$ at High Magnetic Fields," Phys. Rev. B. 41, 8229-8239 (1990).

8. I.M. Tsidilkovski, G.I. Harus and N.G. Shelashina, "Impurity States and Electron Transport in Gapless Semiconductors," Advances in Physics 34, 43-174 (1985).

9. J.R. Lowney, A.H. Kahn, J.L. Blue, and C.L. Wilson, "Disappearance of Impurity Levels in Silicon and Germanium Due to Screening," J. of Applied Phys. 52, 4075-4080 (1981).

10. H.P. Hjalmarson, P. Vogl, D.J. Wolford and J.D. Dow, Theory of Substitutional Deep Traps in Covalent Semiconductors," Phys. Rev. Letters 44, 810-813 (1980).

11. A.J. Syllaios and M.J. Williams, "Conductivity type conversion in (Hg, Cd) Te," J. Vac. Sci. Technol. 21 (1), 201-204 (1982).

12. C.A. Swarts, M.S. Daw, and T.C. McGill, "Bulk vacancies in CdxHg1-xTe," J. Vac. Sci. Technol. 21 (1), 198-200 (1982).

13. S.T. Pantelides, "The electronic structure of impurities and other point defects in semiconductors," Rev. Modern Phys. 50, 797-858 (1978).

B. Electron-Longitudinal Optic Mode Scattering

We have studied the Random Element Isodisplacement Model of two-mode behavior. We have also reviewed models for establishing criteria for two mode versus one mode behavior. We have studied effective charges and their meaning for scattering electrons. We have also reviewed the literature. All of these things are discussed in more detail below.

1. Szigeti, Transverse and Callen Effective Charge

Ionic polarizability is caused by the displacements of the ions as a whole while electronic polarizability is caused by the displacement of the electron cloud relative to the nuclei. The displacement of the ions changes the interatomic distance which in turn affects the distribution of the electron cloud. This effect is a short range interaction, since it only depends on the displacement of the near neighbors. There is another type of interaction between atomic and electronic polarizations through the internal field. This effect is a long range effect since the distant dipoles as well as the near dipoles contribute.

Szigeti defined a correction factor s for deviation from heteropolar behavior as a result of mutual distortions of neighboring ions due to their overlapping. Szigeti charge represents the short range interaction of the electronic and atomic displacements. One might expect to find s very different from one if the ions penetrate considerably into each other or if the bond has partial homopolar character and its polarity changes rapidly with the distance between the atoms. Szigeti has shown how the factor s can be obtained in terms of values that can all be experimentally measured.

The transverse charge is defined to give the local polarization (electronic and atomic) caused by relative displacements. The polarization includes that due to ionic motion and that induced in the electronic charges in the absence of electric fields. The resulting field which scatters electrons is accounted for by separately dividing by ϵ_o (giving rise to the definition of the Callen charge).

The Szigeti effective charge $e_s = se$ is used in computing the force on a ion. Distortion of the charge affects the value of e_s and causes $s \neq 1$. The distortion is due to overlap. By Born and Huang

$$P = \frac{1}{v_\alpha} \{ sze\,(u_+ - u_-) + (\alpha_+ + \alpha_-) \frac{4\pi}{3} P$$

Assuming E = 0, $\alpha \pm$ are the polarizability of the ions and $u_+ - u_-$ is the relative displacement of the ions, z is the charge of the ions and v_α is the volume per molecule. Solving for $\vec{P}$ gives us

$$P = \frac{1}{v_\alpha} \frac{sze\,(u_+ - u_-)}{1 - \frac{4\pi}{3v_\alpha}(\alpha_+ + \alpha_-)}$$

Then using the Clausius-Mosotti equation

$$\frac{4\pi}{3}(\alpha_+ + \alpha_-) = \frac{\epsilon_\infty - 1}{\epsilon_\infty + 2} v_\alpha$$

This means that the polarization can be written

$$P = \frac{1}{v_\alpha} \frac{sze}{3}(\epsilon_\infty + 2)(u_+ - u_-)$$

The quantity

$$e_T = \frac{\epsilon_\infty + 2}{3} se = \frac{\epsilon_\infty + 2}{3} e_s$$

is called the transverse charge. Thus

$$P = \frac{z}{v_\alpha} e_T (u_+ - u_-)$$

This P produces a field which scatters electrons. But in calculating this field we must divide by ϵ_∞ since it is long range and the field is affected by other electrons. So

another relevant charge, called the Callen charge is

$$e_c = e_T/\epsilon_\infty .$$

SUMMARY

e_s: The Szigeti Charge $e_s = se$

This is the effective charge used in figuring the force on an ion. Its value is affected by distortion due to overlap. It is a measure of deviation from ideal heteropolar behavior.

e_T: The Transverse Effective Charge $e_T = \frac{\epsilon_\infty + 2}{3} e_s$

This is defined so as to give local polarization induced by relative displacement. We are interested in induced polarization in the absence of electric fields.

e_c: The Callen Effective Charge $e_c = e_T/\epsilon_\infty = \frac{\epsilon_\infty + 2}{3\epsilon_\infty} e_s$

Note for rigid ions $\epsilon_\infty = 1$ and $e_c = e_T = e_s$.

2. One and Two Mode Behavior

In binary alloy systems, lattice vibration spectra can show two different behaviors. The first is "one mode behavior" in which the phonon frequency changes continuously from the value that corresponds to one end member to that of the other end member with an approximately constant strength. The second is "two mode behavior" in which two frequencies occur with a strength approximately equal to the fractional composition of each component.

Experimentally, this behavior can be seen through infrared and Raman spectroscopy. A Kramers-Kronig dispersion analysis can be applied to reflection spectra to get the real part of the dielectric constant Re $\epsilon(\omega)$, the imaginary part of the dielectric constant Im $\epsilon(\omega)$, and the imaginary part of the reciprocal of the dielectric constant -Im $(1/\epsilon(\omega))$. From these functions the frequencies of the transverse optical phonons (TO) and those of longitudinal optical (LO) phonons are determined . The frequencies of the TO phonons are determined from the positions of the maxima of the Im $\epsilon(\omega)$ curve and the frequencies of the LO phonons from the positions of maxima of -Im $(1/\epsilon(\omega))$ or from the points where the Re $\epsilon(\omega)$ curve crosses the ω - axis. In the case of the two mode behavior, the Kramer-Kronig analysis yields for each x - value two frequencies of the transverse optical phonons (TO_1 and TO_2) and two frequencies of the longitudinal optical phonons (LO_1 and LO_2).

Now returning to the ideas of one and two mode behavior. Consider the pseudobinary compound $AB_{1-x}C_x$ composed of atoms A, B, and C. Two mode behavior in $AB_{1-x}C_x$ may also be seen experimentally in reflectivity spectra. Supposedly, this means the interactions of a cation with one anion and a cation with another anion are independent, thus the AB and AC vibrations are independent. Actually one may see one or two mode behavior depending on the situation.

In one mode behavior the frequencies of long wave length phonons vary continuously from x = 0 (AB) to x = 1 (AC).

In two mode behavior one has two sets of phonon frequencies for each $x \neq 0$ or 1. The set that starts from x = 0 starts from AB type behavior and the set from x = 1 starts from BC type behavior. The mole fractions of AB and AC determine by proportionality the strength of the frequencies.

A sketch of the two kinds of behavior looks like:

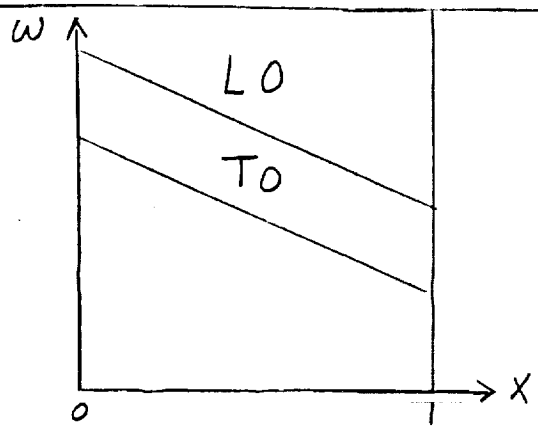

ONE MODE BEHAVIOR

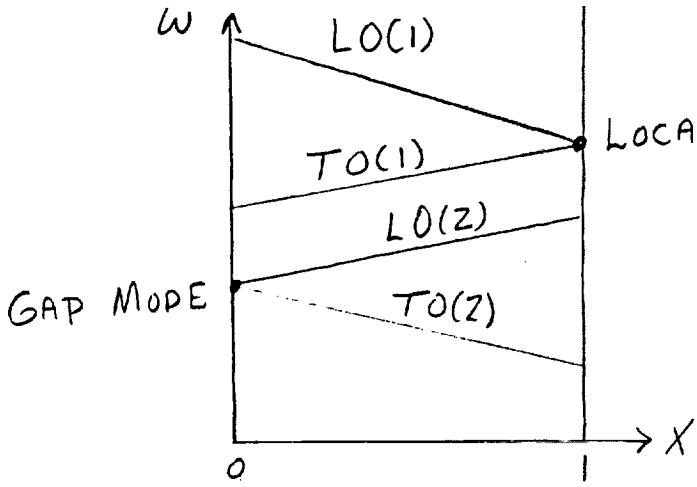

TWO MODE BEHAVIOR

The following convention is used in naming modes. An impurity mode lying above the optic band of the host lattice is a local mode. Note this occurs at $x = 1$. A gap mode lies below the band of the host lattice. Note this occurs at $x = 0$. There are also more complicated situations. Obviously one can reverse directions by letting $x \rightarrow x' = 1-x$, $1 - x \rightarrow x'$.

The actual criteria for one - and two- mode behavior can be somewhat complicated.

Let

$$\epsilon = 1 - M'/M$$

where	$M' > M$	$\epsilon < 0$
and for	$M' < M$	$0 < \epsilon < 1$.

Insight into the times when we should expect two mode behavior and one mode behavior can be gained by considering the vibrational behavior of a one dimensional linear diatomic chain.

If we substitute for the lighter mass with an even lighter impurity (so $\epsilon > 0$) a localized mode will rise out of the top of the optical band. If we substitute with a heavier mass ($\epsilon < 0$) an optical gap mode falls out of the bottom of the same optical branch. If we substitute for the heavier mass with $\epsilon > 0$, then a local mode rises from the top of the optical branch and a gap mode rises out of the top of the acoustical branch. If one substitutes for the heavier mass with $\epsilon < 0$, no new gap or local modes appears. Obviously, one needs local and gap modes for two mode behavior.

Chang and Mitra give the following conditions:

I. $M_B < \mu_{AC}$ so $M_B < M_A$ and M_C (assuming $M_B < M_C$ for $AB_{1-x}C_x$)

or

II. $M_C < \mu_{AB}$ so $M_C < M_A$ and M_B (assuming $M_C < M_B$ for $AB_{1-x}C_x$)

If (I.) or (II.) is satisfied, then $AB_{1-x}C_x$ is two mode, otherwise it is one mode.

3. The random element isodisplacement model

There are several models for calculations in mixed crystal systems. In a virtual crystal model all masses and spring constants are taken to have the same average value.

Verleur and Barker have accounted for two mode behavior in some mixed crystals using a model based on short range clustering.

This is a good working model proposed by Chen and developed by Chang and Mitra to account for two mode behavior in crystals of the form $AB_{1-x}C_x$ where x gives the concentration of C relative to A. See Gorska and Nazarewicz. There are two basic assumptions

(a) All atoms of the same kind move together (isodisplacement).

(b) We can think of the crystal as having two sublattices. One is a lattice of atoms of the type A and the other is a random distribution of atoms of the type B and C with relative concentrations 1-x and x.

Let m_A, m_B, m_C be the masses of the atoms, u_A, u_B, u_C be the displacements from equilibrium, e_A, e_B, e_C be the effective charges of the ions, $\mathbf{E}_{eff}$ be the effective field, and F_{AB}, F_{AC}, and F_{BC} be the force constants.

Thus we can write:

$$M_A\ddot{U}_A = -(1-x)F_{AB}(U_A - U_B) - xF_{AC}(U_A - U_C) + e_A E_{eff} \tag{1a}$$

$$M_B\ddot{U}_B = -F_{AB}(U_B - U_A) - xF_{BC}(U_B - U_C) - e_B E_{eff} \tag{1b}$$

$$M_C\ddot{U}_C = -F_{AC}(U_C - U_A) - (1-x)F_{BC}(U_C - U_B) - e_C E_{eff} \tag{1c}$$

We assume a linear dependence of the force constants on the composition:

$$\frac{F_{AB}}{F_{ABO}} = \frac{F_{AC}}{F_{ACO}} = \frac{F_{BC}}{F_{BCO}} = 1 - \theta x \tag{2}$$

The effective charges must be determined by the electrical neutrality condition:

$$e_A - (1-x)e_B - xe_c = 0. \tag{3}$$

We start out by looking at long-wavelength transverse optical phonons for which $E \approx 0$. For this case

$$P = N [e_A U_A - (1 - x) e_B U_B - x e_C U_C] + N_\alpha E_{eff} \tag{4a}$$

where

$$E_{eff} = E + \frac{4\pi}{3} P = \frac{4\pi}{3} P \tag{4b}$$

The electronic polarizability is determined by the Clausius-Mossotti equation

$$\frac{4\pi}{3} N\alpha = \frac{\epsilon_\infty - 1}{\epsilon_\infty + 2} \tag{5}$$

Using Eqs. (4a), (4b) and (5) we find:

$$P = \frac{\epsilon_\infty + 2}{3} N [e_A U_A - (1 - x) e_B U_B - x e_C U_C] \tag{6}$$

and

$$E_{eff} = \frac{4\pi}{3} \frac{\epsilon_\infty + 2}{3} N [e_A U_A - (1 - x) e_B U_B - x e_C U_C] \tag{7}$$

Using Eq. (3), Eq. (7) becomes:

$$E_{eff} = \frac{4\pi}{3} \frac{\epsilon_\infty + 2}{3} N [(1 - x) e_B (U_A - U_B) + x e_C (U_A - U_C)]$$

Repeated use of Eq. (3) allows us to express E_{eff} as involving $(U_A - U_B)$, $(U_B - U_C)$, or $(U_C - U_A)$, $(U_C - U_B)$.

$$M_A \ddot{U}_A = - (1 - x) F'_{AB} (U_A - U_B) - x F'_{AC} (U_A - U_C) \tag{8a}$$

$$M_B \ddot{U}_B = + F'_{AB} (U_A - U_B) - x F'_{BC} (U_B - U_C) \tag{8b}$$

$$M_C \ddot{U}_C = F'_{AC} (U_A - U_C) + (1 - x) F'_{BC} (U_B - U_C) \tag{8c}$$

where

$$F'_{AB} = F_{AB} - \frac{4\pi}{3}\,\frac{\epsilon_\infty + 2}{3}\,N\,e_A\,e_B \tag{9a}$$

$$F'_{AC} = F_{AC} - \frac{4\pi}{3}\,\frac{\epsilon_\infty + 2}{3}\,N\,e_A\,e_C \tag{9b}$$

$$F'_{BC} = F_{BC} + \frac{4\pi}{3}\,\frac{\epsilon_\infty + 2}{3}\,N\,e_B\,e_C \tag{9c}$$

Now defining

$$W_1 = U_A - U_B \tag{10a}$$

$$W_2 = U_B - U_C \tag{10b}$$

$$W_1 + W_2 = U_A - U_C \tag{10c}$$

The equations become:

$$\ddot{W}_1 = -(K_1 + K_{12})\,W_1 - K_{12}W_2 \tag{11a}$$

$$\ddot{W}_2 = (K_1 - K_2 + K_{12} - K_{21})\,W_1 - (K_2 - K_{12})\,W_2 \tag{11b}$$

where

$$K_1 = (1 - x)\,\frac{F'_{AB}}{M_A} + \frac{F'_{AB}}{M_B} + x\,\frac{F'_{BC}}{M_B} \tag{12a}$$

$$K_2 = x\,\frac{F'_{AC}}{M_A} + \frac{F'_{AC}}{M_C} + (1 - x)\,\frac{F'_{BC}}{M_C} \tag{12b}$$

$$K_{12} = x\,\frac{F'_{AC}}{M_A} - x\,\frac{F'_{BC}}{M_C} + (1 - x)\,\frac{F'_{BC}}{M_C} \tag{12c}$$

$$K_{21} = (1 - x)\frac{F'_{AB}}{m_A} - (1 - x)\frac{F'_{BC}}{m_C} \tag{12d}$$

Thus

$$\omega^4 - (K_1 + K_2)\,\omega^2 + (K_1K_2 - K_{12}K_{21}) = 0 \tag{13}$$

We now redo this for the case of longitudinal optical phonons with $\epsilon = 0$, or the more familiar form $E = -4\pi P$. This is given by Kittel (p. 275) and follows from

$P = \frac{\epsilon - 1}{4\pi} E$ with $\epsilon = 0$. Using

$$E = -4\pi P, \tag{14}$$

$$E_{eff} = E + \frac{4\pi}{3} P$$

$$= -\frac{8\pi}{3} P \,. \tag{15}$$

Combining Eqs. (15), (5) and (4a), we find:

$$P = \frac{\epsilon_\infty + 3}{3\epsilon_o}\left(e_A U_A - (1 - x)\, e_B U_B - x\, e_C U_C\right) \tag{16a}$$

$$E_{eff} = -\frac{8\pi}{3}\,\frac{\epsilon_\infty + 3}{3\epsilon_o}\left(e_A U_A - (1 - x)\, e_B U_B - x\, e_C U_C\right) \tag{16b}$$

Thus we find

$$M_A\ddot{U}_A = -(1 - x)\,F''_{AB}(U_A - U_B) - x\,F''_{AC}(U_A - U_C) \tag{17a}$$

$$M_B\ddot{U}_B = -F''_{AB}(U_B - U_A) - x\,F''_{BC}(U_B - U_C) \tag{17b}$$

$$M_C\ddot{U}_C = -F''_{AC}(U_C - U_A) - (1 - x)\,F''_{BC}(U_C - U_B) \tag{17c}$$

where

$$F''_{AB} = F_{AB} + \frac{8\pi}{3} N e_A e_B \left(\frac{\epsilon_\infty + 2}{3\epsilon_\infty}\right) \tag{18a}$$

$$F''_{AC} = F_{AC} + \frac{8\pi}{3} N e_A e_C \left(\frac{\epsilon_\infty + 2}{3\epsilon_\infty}\right) \tag{18b}$$

$$F''_{BC} = F_{BC} - \frac{8\pi}{3} N e_B e_C \left(\frac{\epsilon_\infty + 2}{3\epsilon_\infty}\right). \tag{18c}$$

Thus we have the same equation for transverse and longitudinal optic phonons, except that F''_{AB} replaces F'_{AB}.

We assume that N and ϵ_∞ depend on x as follows:

$$N = (1 - x)\, N_{AB} + x\, N_{AC} \tag{19a}$$

$$\epsilon_\infty = (1 - x)\, \epsilon_{\infty,\,AB} + x\, \epsilon_{\infty,AC} \tag{19b}$$

and we also assume

$$e_B = e^*_{AB} \tag{20a}$$

$$e_C = e^*_{AC} \tag{20b}$$

so $$e_A = (1 - x)\, e^*_{AB} + x\, e^*_{AC} \tag{20c}$$

where e* is the Szigeti effective charge. Now it is a matter of solving Eq. (13).

Summary for crystals of the form $AB_{1-x}C_x$, we need to solve Eq. (13) for ω^2 with the K_i's defined by Eq. (12) in which the F''s are replaced by F'''s with Eq. (20) used. The solution gives ω^2 as a function of x.

For the spherical case of long wavelength optical phonons at x = 0 and x = 1, we find the following initial conditions.

$x = 0$

$$\omega^2_{LO\ AB} = \frac{F_{ABO}}{\mu_{AB}} + \frac{8\pi}{3}\ \frac{N_{AB}\,(e^{*}AB)^2}{\mu_{AB}}\left(\frac{\epsilon_{\infty,\,AA} + 2}{3\epsilon_{\infty,\,AB}}\right)$$

$$\omega^2_{gap,\,AB} = \frac{F_{ACO} + F_{BCO}}{M_C}$$

$x = 1$

$$\omega^2_{LO\ AC} = \frac{F_{ACO}\,(1 - \theta)}{\mu_{AC}} + \frac{8\pi}{3}\ \frac{N_{AC}\,(e^{*}AC)^2}{\mu_{AC}}\left(\frac{\epsilon_{\infty,\,AC} + 2}{3\epsilon_{\infty,\,AC}}\right)$$

$$\omega^2_{local,\,AC} = \frac{F_{ABO} + F_{BCO}}{M_B}\,(1 - \theta)$$

where $\frac{1}{\mu_{AB}} = \frac{1}{M_A} + \frac{1}{M_B}$ and $\frac{1}{\mu_{AC}} = \frac{1}{M_A} + \frac{1}{M_C}$.

There is also the question as to whether the two mode theory for photon scattering is the same as the two mode theory needed for electron scattering. One might say that the Green's function for scattering in the two cases would be clearly different. However we are interested in long wavelength modes mostly, and at any rate the Green's function probably depends more on frequency than wave vector. Thus we assume our approximation is not a bad one. This is especially true because we assume each optic mode only has one frequency which is independent of wave vector.

SELECTED REFERENCES

1. M.P. Volz, F.R. Szofran, S.L. Lehoczky and Ching-Hua Su, "Lattice Vibration Spectra of $Hg_{1-x}Zn_xTe$ Alloys," Solid State Communications 75, 943-947 (1990).

2. M. Gorska and W. Nazarewicz, "Application of the Random-Element Isodisplacement Model to Long-Wavelength Optical Phonons in $CdSe_xTe_{1-x}$ Mixed Crystals," phys. stat. sol. (b) 65, 193 (1974).

3. J. Baars and F. Sorger, "Restralen Spectra of HgTe and $CdHg_{1-x}Te$," Solid State Communications, Vol. 10, pp. 875-878, 1972.

4. I.F. Chang and S.S. Mitra, "Long Wavelength Optical Phonons in Mixed Crystals," Adv. Phys. 20, 359-404 (1971).

5. I.F. Chang and S.S. Mitra, "Application of a Modified Random-Element-Isodisplacement Model to Long-Wavelength Optic Phonons of Mixed Crystals," Phys. Rev. 172, 924 (1968).

6. Y.S. Chen, W. Shockley, and G.L. Pearson, "Lattice Vibration Spectra of $GaAs_x P_{1-x}$ Single Crystals," Phys. Rev. 151, 648-656 (1966).

7. H.W. Verleur and A.S. Barker Jr., Phys. Rev. 149, 715 (1966).

In the following graph we plot MCT mobility versus temperature for several different values of transverse charge which have appeared in the literature. The main difference appears at intermediate temperature where variations of 10% or so can be seen. See also the accompanying table where numbers and references to the values of transverse charge are given. It seems clear that the effective charge determining the strength of scattering is not rigorously determined. However, different reasonable choices seem to have little effect on the mobility vs. temperature.

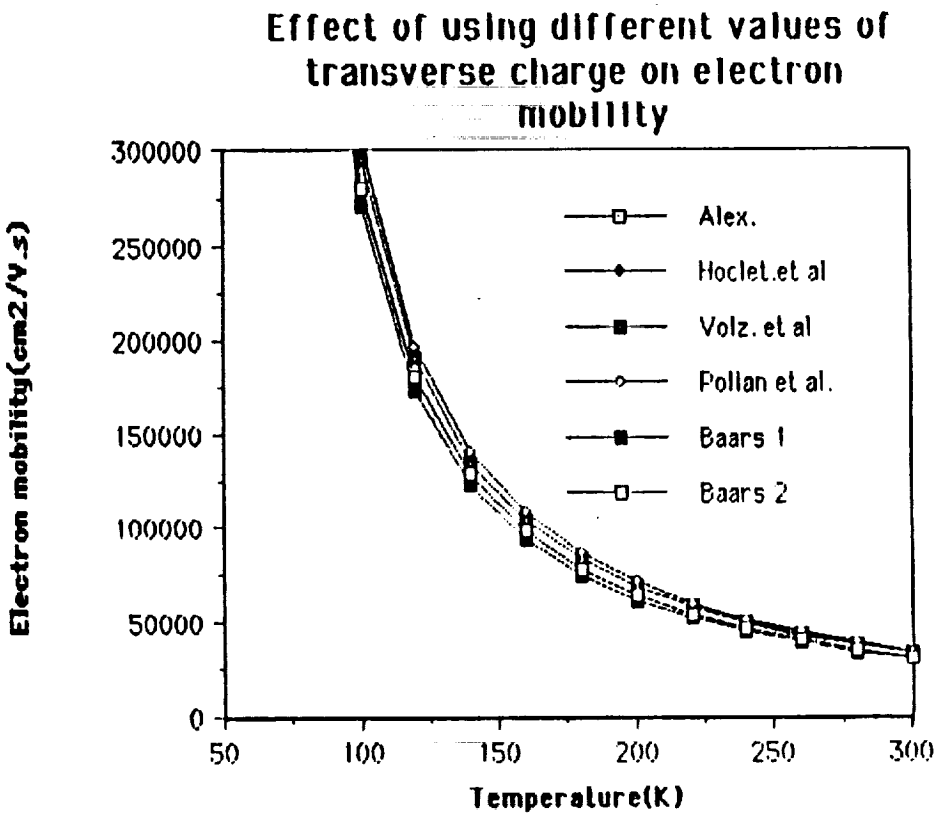
Effect of using different values of transverse charge on electron mobility
Electron mobility(cm2/V.s)
300000
250000
200000
150000
100000
50000
0
50
100
150
200
250
300
Temperature(K)
Alex.
Hoclet.et al
Volz. et al
Pollan et al.
Baars 1
Baars 2

$X = 0.193$

	Temp.	Alex.	Hoclet.et al	Volz. et al	Polian et al.	Baars 1	Baars 2
1	60.000	751076.988	784033.540	784824.112	779743.921	745762.683	751620.406
2	80.000	474669.724	493102.113	494049.558	504562.754	465220.325	475571.316
3	100.000	281514.659	295403.722	296080.181	304674.154	271577.235	280418.237
4	120.000	180222.338	190577.704	191046.739	197450.278	173138.017	180278.574
5	140.000	128833.736	135450.259	135788.053	141634.843	122946.166	128853.993
6	160.000	98241.851	104473.185	104729.670	108572.000	94170.610	98234.536
7	180.000	77950.747	83773.962	83976.153	87068.487	75207.492	77915.401
8	200.000	65094.544	69196.174	69359.012	71893.737	62144.293	65077.605
9	220.000	54977.009	58386.936	58520.214	60613.609	52537.899	54960.132
10	240.000	47153.305	50002.296	50112.731	51862.702	45074.538	47137.175
11	260.000	40917.205	43317.087	43406.770	44867.309	39147.968	40902.063
12	280.000	35825.421	37869.652	37947.938	39199.175	34318.862	35812.109
13	300.000	31590.175	33362.540	33429.177	34496.583	30287.202	31578.142
14	320.000	28069.279	29574.540	29636.356	30549.166	26942.153	28058.859
15	340.000	25048.543	26373.168	26422.784	27225.181	24088.784	25039.744
16	360.000	22488.594	23628.672	23673.498	24365.650	21631.696	22480.530

AUTHOR	e_T/e (HgTe)	e_T/e(CdTe)	REFERENCE
Alex	2.96	2.35	S.L. Lehoczky, F.R. Szofran and B.G. Martin, "Advanced Methods for Preparation and Characterization of Infrared Detector Materials, Part I," NASA CR-161598, Page 70, July 5, 1980.
Hoclet	2.72	2.27	phys. stat. sol (b) 92, 545, (1979)
Volz	2.72	2.239	Solid State Comm., Vol. 75, No. 12, pp. 943-947, 1990
Polian	2.52	2.38	Phys. Rev. B, Vol. 13, Number 8, 1976
Baars	3.2	2.245	Solid State Communic., Vol. 10, pp. 875-878, 1972
Baars	2.981	2.287	Solid State Communic., Vol. 10, pp. 875-878, 1972

used $e_T^* = \frac{\epsilon_\infty + 2}{3} e_s^*$

Reference →Lucovsky et al., Phys. Rev. B, Vol. 4, Number 4, 1367-1371, 1971.

C. Review of Alloy Disorder Scattering

The alloy Hamiltonian can be written, in an approximation, as a uniform virtual Hamiltonian with a residual alloy disorder potential. The virtual crystal approximation is used in alloys which are formed by ternary solid solutions between II-VI binary compounds. In the virtual crystal approximation (VCA) the actual non periodic structure is replaced by an average which is periodic. We consider a crystal of the form $A_xB_{1-x}C$. The lattice of the atoms A is fcc and the lattice of the B, C atoms randomly occupy a second fcc lattice. Thus in VCA, the random potential, created by $B(V_B)$ and $C(V_C)$ atoms is not used. Instead, a periodic potential which is the weighted averages of these two is appropriate. In equation form, we write

$$< V > = V_A + x V_C + (1 - x) V_B.$$

The use of the average potential leads again to Bloch waves and effective masses, but the residual disorder then leads to scattering between the Bloch waves and to a compositional dependence of the band gaps. Only when the two binaries making up the pseudobinary alloy have very similar band structure and lattices, does the band gap vary approximately linearly with composition. After analysis, this typically leads to a scattering term proportional to x(1-x), however things are really not so simple as one needs to know with what strength to treat this scattering term. The answer that is usually given is that the strength is proportional to the difference between two band widths. For example in MCT, the difference in the bandwidth between HgTe and CdTe. Kossut has looked at the scattering in more detail and finds that it actually depends on three matrix elements involving the difference in potential between Hg and Cd. The one involving the spin-orbit interaction is apparently zero for MCT, the other two, are not necessarily zero. Only when two of the three are zero is the scattering proportional to the difference in the band gap energies from HgTe and CdTe. One further problem is the non uniformity of the disorder via, for example, clustering.

SELECTED REFERENCES

1. M.A. Berding, S. Krishnamurthy, and A. Sher, "Electronic and Transport Properties of HgCdTe and HgZnTe," J. Vac. Sci. Technol. 5A, 26-30 (1987).

2. K.C. Hass, R.J. Lempert, and H. Ehrenreich, "Effects of Chemical and Structural Disorder in Semiconducting Pseudobinary Alloys," Phys. Rev. Letters 52, 77-80 (1984).

3. D.S. Montgomery, "Disorder Scattering and Electron Mobility in $Hg_{1-x}Cd_xTe$," J. Phys. C : Solid State Physics 16 , 2923-2934 (1983).

4. J. Kossut, "The Disorder Scattering in Zincblende Narrow-Gap Semiconduction Mixed Crystals," phys. stat. sol. (b) 86 , 593 (1978).

5. L. Makowski and M. Glicksman, "Disorder Scattering in Solid Solutions of III-V Semiconducting Compounds," 34, 487-492 (1973).

D. Other Scattering Mechanisms

Obviously dislocations are imperfections in the crystal and as such they can act as scattering centers. For example, edge dislocations create strain fields which can scatter electrons due to coupling to the deformation potential. Dislocations can also become charged and thus act as scattering centers due to their charge which may be screened by free carriers or impurities or both. A discussion of dislocation scattering has been given by Zawadzki. It should be pointed out that this subject is not only of academic interest. Pelliciari, Destefanis, and DiCioccio have found evidence of anomalous behavior in low n type mercury cadmium telluride induced by extended defects. Their samples have shown a kink in the mobility curve between 77 and 100 K. Transmission Electron Microscopy experiments have correlated this kink with the appearance of dislocations and a significant decrease in the mobility. A very serious practical problem is the effect of temperature gradients on dislocation formation during crystal growth.

SELECTED REFERENCES

1. B. Pelliciari, G.L. Destefanis, and L. DiCioccio, "Evidence of anomalous behavior in low n-type mercury cadmium telluride induced by extended defects," J. Vac. Sci. Technol. A7 (2), 314-320 (1989).

2. W. Zawadzki, "Mechanisms of Electron Scattering in Semiconductors," Handbook on Semiconductors Vol. 1, Ch. 12 North-Holland Publ. co. (1982).

E. Further Work in MZT

The best summary of further work on MZT that we have done has been summarized in a recent paper by us which appeared in the August issue of the Journal of Materials Research. One of the main results of this paper is a comparison of our work with experimental work done by others. We should also mention that although MZT has several advantages as a IR detector (over MCT) primarily because of its increased Hg stability it also suffers from a greater difficulty in growing uniform crystals. This is because less Zn than Cd is needed for a given E_g and $\frac{dE_g}{dx}$ for E's of interest is greater for MZT. Thus small errors in x are magnified in energy gap fluctuations.

SELECTED REFERENCES

1. J.D. Patterson, Wafaa A. Gobba, and S.L. Lehoczky, "Electron Mobility in n-Type $Hg_{1-x}Cd_xTe$ and $Hg_{1-x}Zn_xTe$ Alloys," J. Materials Research 7 (August 1992) to be published.

2. Wafaa Abdelhakiem and J.D. Patterson, "A comparison between electron mobility in n-type $Hg_{1-x}Cd_xTe$ and $Hg_{1-x}Zn_xT$," Materials Letters 11, 47-51 (1991).

3. E.A. Patten, M.H. Kalisher, G.R. Chapman, J.M. Fulton, C.Y. Huang. P.R. Norton, M. Ray and S. Sen, "HgZnTe for very long wavelength infrared applications," J. Vac. Sci. Technol. B9(3), 1746-1751 (1991).

4. G. Le Bastard, R. Granger, S. Rolland, Y. Marqueton, and R. Triboulet, "Optical Vibration Models in $Hg_{1-x}Zn_xTe$Solid Solutions near q = 0," J. Phys. France 50 3223-3232 (1989).

5. R. Granger and C.M. Pelletier, "Electron Mobility Evaluation in $Hg_{1-x}Cd_xTe$ and $Hg_{1-x}Zn_xTe$ with Two Mode Optical Dispersion," Presented at 5th Int. Cong. on II-VI Compounds, Yokagama, Japan.

6. S. Rolland, A. Lasbley, A. Seyni, R. Granger, and R. Triboulet, "Electrical Characterization of as-grown, annealed, and indium-doped $Hg_{1-x}Zn_xTe$ for x near 0.15, "Revue Phys. Appl. 24, 795-802 (1989).

7. R. Granger, A. Lasbley, S. Rolland, c.M. Pelletier, and R. Triboulet, "Carrier Concentration and Transport in $Hg_{1-x}Zn_xTe$ for x near 0.15," J. Crystal Growth 86, 682-688 (1988).

F. Experimental Data

Experimental data on narrow gap materials other than MCT is relatively sparce. Besides the references given in E we note the papers by M. Voltz et al noted in B.

We have also "invented" some materials by changing the parameters of MZT and MCT by factors which are arbitrary but not totally unreasonable. The idea was to check if a more or less random but reasonable set of parameters would fit experiment as well as any. Happily they did not for otherwise we would have to say that our good results were fortuitous.

Other references include:

1. S.D. Cobb, R.N. Andrews, F.R. Szofran, and S.L. Lehoczky, "Characterization of Directionally Solidified MErcury Zinc Selenide Semiconducting Alloys," J. Cryst. Growth 110 (3) 415-22 (1991).

2. K. Kumazaki, "Dielectric Constant of Zinc Mercury Selenide ($Zn_xHg_{1-x}Se$) Determined by Raman Scattering," phys. stat. solids B, 160 , K173-176 (1990).

3. K. Kumazaki, "Resonant Raman Scattering in Zinc Mercury Selenide," phys. status solidi B 183 , 751-6 (1989).

4. K. Kumazaki, L. Vina, C. Unbach, M. Cardona, "Interband Critical Point Parameters Determined by Ellipsometry in Zinc Mercury Selenide," Solid State Commun. 68 , 591-4 (1988).

5. K. Kumazaki, "Optical Damping Constants due to Free Carriers in Narrow Gap Semiconductors," Solid State Commun. 64 , 567-7 (1987).

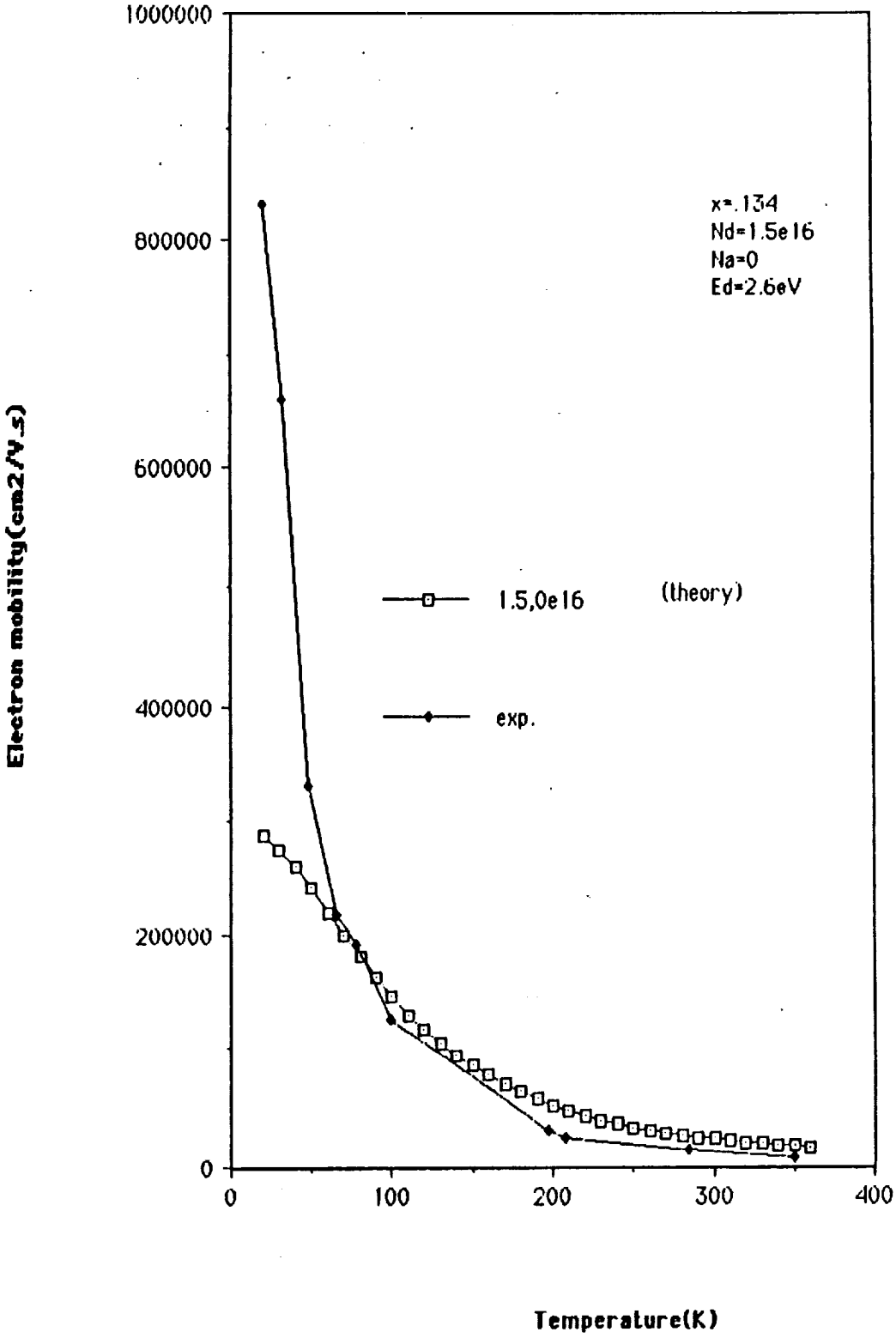

Fig. 7. A comparison between theoretical and experimental results for MZT electron mobility.

G. Superlattices

We have several comments to make about superlattices. Unfortunately experimental studies require sophisticated equipment such as a molecular beam epitaxy apparatus.

A superlattice (SL) which has alternating layers of CdTe and HgTe has been proposed by Schulman and McGill as a new IR material which can be made by molecular beam epitaxy. The first successful molecular beam epitaxy growth of a Hg-Te superlatttice occurred in 1982. The band gap depends on the width of the quantum wells as well as the barrier width and height. Thus the formation of HgTe/CdTe superlattices allow a good control of the bandgap (in fact better than obtained in the growth of alloys) which can be a variable from zero to about 1.6 eV. We have also done some rough modeling of high mobility devices which are based on doping in the barrier to furnish electrons to the quantum wells. Some results are given below. Representative references are listed.

There are several comments one could make about the utility of superlattices as IR detectors. In some ways superlattices are an advantage. For one, the energy gap versus SL well layer thickness d_w can be better controlled in SL's than E_g versus x in bulk crystals - at least for E_g's of interest. This is particularly true because the cut off wavelength for E_g's of interest is a much more rapidly varying function of x for bulk crystals than of the layer thickness for superlattices.

There exists a neat trick (Stormer and Dingle) in SL's that can be used to increase the number of electrons without reducing the low temperature mobility due to ionized impurity scattering. This is accomplished by adding donors to the barrier region allowing the electrons to fall into the "wells". In calculations dealing with electron mobility in superlattices, it has been found that the temperature dependence of the mobility is greatly affected by interface roughness which leads to complications in making accurate calculations.

There are other advantages to the HgTe-CdTe superlattices as given by Smith, McGill and Schulman. The superlattice tunneling currents are reduced compared to bulk and diffusion currents in photovoltaic devices made from SL's are reduced as is band to band tunneling currents across the junction.

HgTe-ZnTe SL's have also been considered but because of a 6.5% lattice mismatch these become strained layer superlattices. The straining can cause additional effects which may be tailored to advantage. We have also done calculations which model crudely the way mobility can be enhanced by using layered structures consisting of alternate layers of "quantum wells" and barriers.

The electron wave function in superlattices is approximately (1);

$$\psi^{A}_{(\vec{r})} = \Sigma_C \, e^{i\vec{k}_\perp \vec{r}} \, V^{A}_{C\vec{k}}(\vec{r}) \, Xm^{A}_{(z)} \text{ if } \vec{r} \text{ is in an A layer,}$$

and

$$\psi^{B}_{(\vec{r})} = \sum_C e^{i\vec{k}_\perp \vec{r}} \, V^{B}_{C\vec{k}}(r) \, Xm^{B}(z) \quad \text{if } \vec{r} \text{ is in a B layer,}$$

where $k_\perp$ is the direction perpendicular to the z direction (perpendicular to the layers), $V^{A \text{ or } B}_{C\vec{k}}$ is the Bloch wave function for the A or B material, and Xm (z) is the envelope wave function which is given by the Schroedinger equation:

$$\left(- \frac{h^2}{2m^*(z)} \frac{\partial^2}{\partial z^2} + V_c(z) \right) Xm^{A \text{ or } B}_{(z)} = \epsilon_m \; X_{m\,(Z)}^{A \text{ or } B} \,,$$

in a reasonable approximation.

Here, m^* is the electron effective mass of the A or B material, V_C (z) is the energy level of the bottom of the conduction bands and ϵ_m is the energy eigenvalue which represents the confinement energy of the carriers. The boundary conditions at the interfaces between A and B materials are that X_m (z) and $[1/m^*(z)]\,[\partial X_m(z)/\partial z]$ be continuous. The energy levels in the conduction band can be approximated by the Kane model for describing the electrons and holes in the A and B materials. Further details are given in Bastard (2).

In general the question of energy bands in superlattices is very complicated. For one situation, once can picture the parabolic quarter wells as splitting the original A or B bands into mini bands. One of the most controversial items in band structure determinations is the value of the valence band offset. There is also band bending which can occur when charge is transferred between barriers and wells.

In the following graphs we have done a calculation which models very crudely the way that mobility can be enhanced by using layered structures consisting of alternate layers of quantum wells and barriers. If one adds donors in the barriers the resulting electrons will drift to the quantum well resulting in more electrons without more scattering centers. The actual calculation we have done keeps the number of electrons constant and reduces the number of scattering centers. Thus the low temperature mobility (parallel to the layers) would be increased. In the following graphs slt = 10 means we have N_d electrons at low temperatures with only $N_d/10$ ionized impurities/volume. Further increase of slt to 100 produces minimal low temperature gain in the mobility. There is no change in the effect for further increase in slt which seems to mean that the effect "saturates" for high electron concentration at low temperature. This would mean that ii impurity scattering has become negligible due to a decrease in ii scattering centers.

A superlattice model for MCT

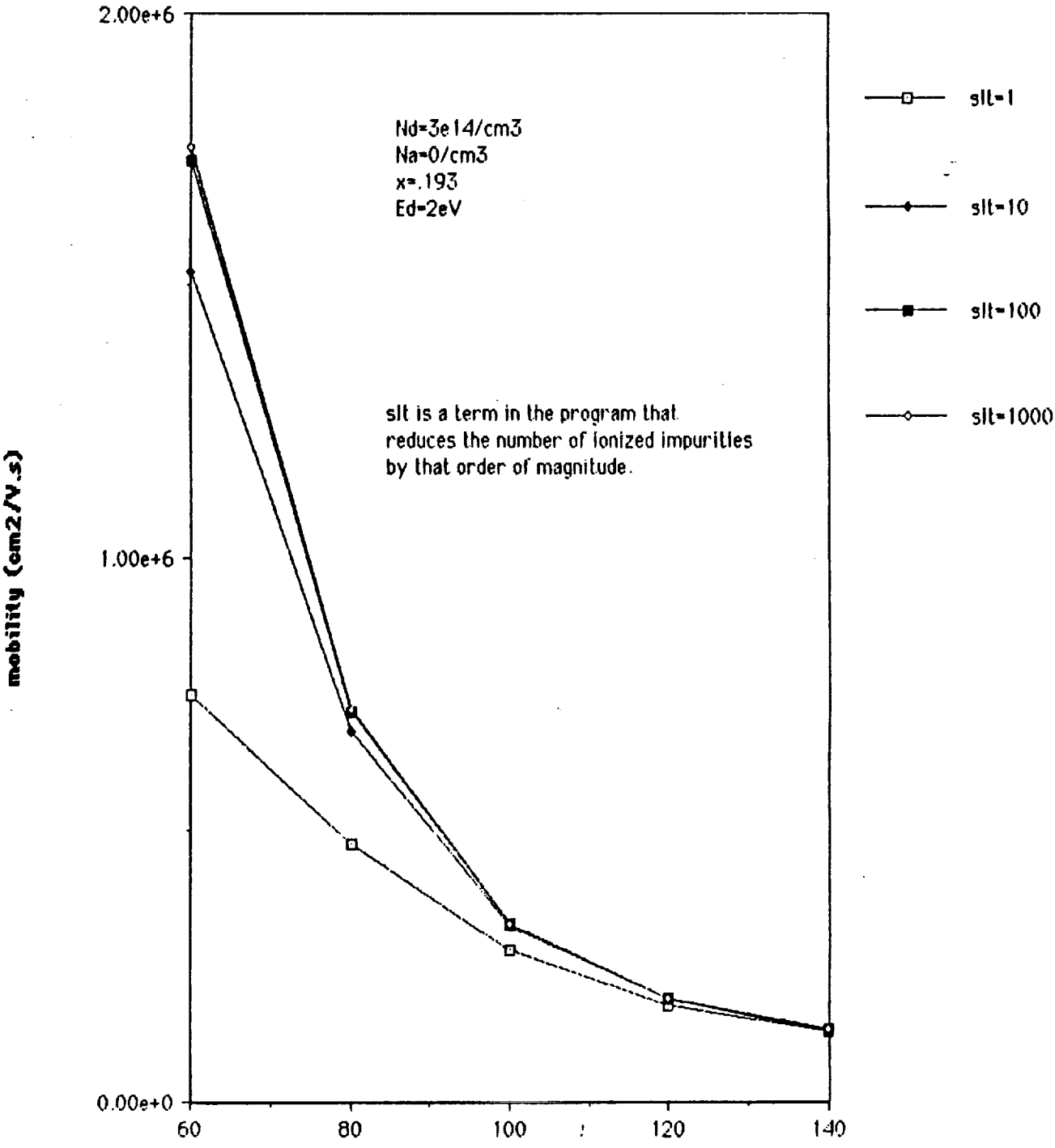

A superlattice model for MZT

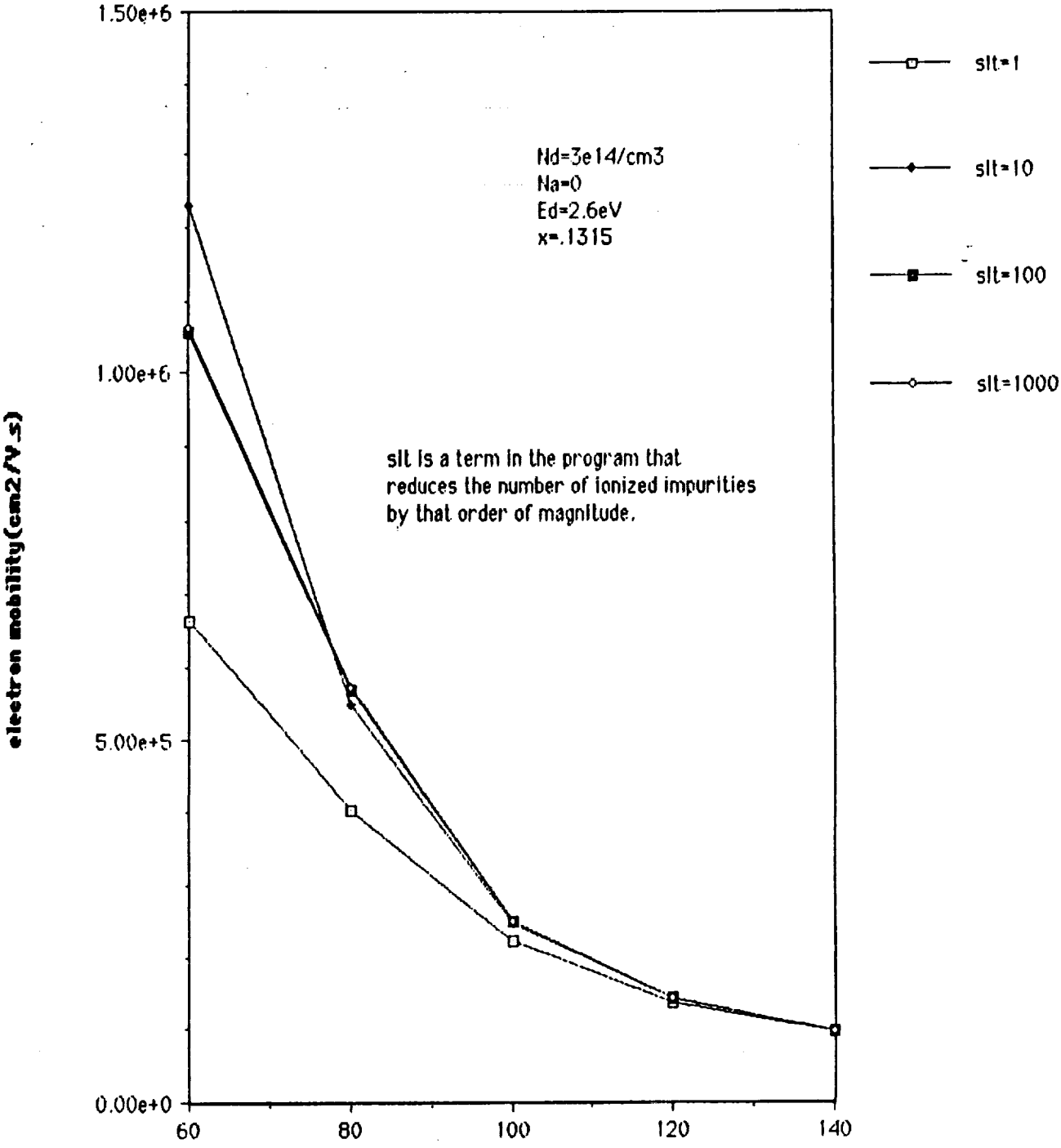

SELECTED REFERENCES

1. C. Weisbuch and B. Vinter, "Quantum Semiconductor Structures," Academic Press, Inc., New York, 1991.

2. J.R. Meyer, D.J. Arnold, C.A. Hoffman, and F.J. Bartoli, "Theory for Electron and Hole Transport in HgTe-CdTeSuperlattices," J. Vac. Sci. Technol. B9(3), 1818-1822 (1991).

3. G. Bastard, J.A. Brun, and R. Ferreira, "Electronic States in Semiconductor Heterostructures" in Solid State Physics Editors Henry Ehrenreich and David Turnbull 44, 229-415 (1991).

4. G. Bastard, "Wave Mechanics Applied to Semiconductor Heterostructures," Halsted Press, New York, 1988.

5. Jean-Pierre Faurie, "Growth and Properties of HgTe-CdTe and Other Hg-Based Superlattices," IEEE Journal of Quantum Electronics, Vol. QE-22(9) 1656-1665 (1986).

6. D.L. Smith, T.C. McGill and J.N. Schulman, "Advantages of the HgTe-CdTe Superlattice as an Infrared Detector Material," Appl. Phys. Lett. 43 (2), 180-182 (1983).

7. J.N. Schulman and T.C. McGill, "The CdTe/HgTe Superlattice: Proposal for a New Infrared Material Appl. Phys. Lett. 34 (10), 663-665 (1979).

H. MMT and Parameter Tables

A preprint of a paper is enclosed which has the parameter tables for MMT and also the results of our mobility calculations.

A comparison between electron mobilities in $Hg_{1-x}Mn_xTe$ and $Hg_{1-x}Cd_xTe$*

Wafaa A. Gobba and J. D. Patterson
Department of Physics and Space Sciences
Florida Institute of Technology
Melbourne, FL 32901-6988 U.S.A

and

S. L. Lehoczky
ES75, Space Science Laboratory
Marshall Space Flight Center, AL 35812 U.S.A.

ABSTRACT

Electron mobility in the n-type diluted magnetic semiconductor $Hg_{1-x}Mn_xTe$ has been calculated in the absence of a magnetic field. The results were compared to those of $Hg_{1-x}Cd_xTe$ for the same range of energy gap. The calculations are based on solving the Boltzman equation using a variational principles technique. The scattering processes that are included in the calculations are the scattering of the electrons with the ionizied impurities, holes, alloy disorder, acoustic phonons and longitudinal optical phonons. At room temperatures the mobilities are nearly the same, while at temperatures of order of liquid nitrogen they are about 30% less for MMT as compared to MCT with the same concentration of defects. $Hg_{1-x}Mn_xTe$ represents a good material for infrared detectors. One of the advantages it has over $Hg_{1-x}Cd_xTe$ is that the band gap changes faster with Mn in $Hg_{1-x}Mn_xTe$ than it does with Cd in $Hg_{1-x}Cd_xTe$ which leads to less scattering due to alloy disorder.

I. Introduction

Although $Hg_{1-x}Cd_xTe$ (MCT) has many problems due to lattice, surface, and interface instabilities[1] it is still a dominant material for use in infrared detectors. Because of the disadvantages of MCT other materials are being studied as better alternatives. One may start the search for new materials by noting that Cd, Zn, Mg and Mn open the band gap of the semimetals HgTe and HgSe[2] and thus produce potential infrared detector materials. $Hg_{1-x}Zn_xTe$ may be superior for use as an infrared detector over $Hg_{1-x}Cd_xTe$ because it is chemically more stable and at the same time shares the same electronic properties[3-7]. $Hg_{1-x}Cd_xSe$ typically shows n-type conductance and does not easily show type conversion[8]. Mg has a stability problem with the Hg-Te bond when the required amount for the 10μm range is introduced[9]. $Hg_{1-x}Mn_xTe$ (MMT) is not a true II-VI alloy but it acts as one. The 3d orbitals of Mn are exactly filled with one electron per orbital and the five spins in these orbitals are parallel, by Hund's rule. It would require about 6-7 eV to add an addition electron with opposite spin to the Mn atom. As a result the $3d^5$ shell acts as if it is complete shell and the Mn atom behaves as a group II element[10].

MMT being a diluted magnetic semiconductor, represents a good material for infrared detectors for the following reasons :

1) $Cd_{1-x}Mn_xTe$ provides a suitable substrate for epitaxial growth due to its lattice constant[11].
2) The band gap changes approximately twice as fast with Mn in MMT as with Cd in MCT. A smaller amount of Mn is needed to produce the same required energy gap which leads to less scattering due to alloy disorder[12]. For detection in the 8-14 μm window 20% CdTe in MCT is needed while only about 11% MnTe in MMT is required.
3) Using a magnetic field, at very low temperatures, the energy gap can be fine tuned due to the presence of the exchange interaction[13].
4) Lattice, surface and interface instabilities[14] in MMT are less when compared to MCT due to the bond stability of Hg-Te.
5) Segregation[15,16] of CdTe in MCT is more of a problem than segregation of MnTe in MMT. Thus MMT is more uniform.

Diluted magnetic semiconductors (DMS) are characterized by the presence of substitutional magnetic ions which causes spin-spin exchange interactions between the localized magnetic moments and the band electrons. This interaction changes the band structure and the impurity states in the presence of a magnetic field. The significance of this interaction has been explained in several review articles[17-21].

Single crystals of MMT have been grown using different techniques: the Bridgman method[22-24], the travelling-solvent method[25], the liquid-phase epitaxy method (LPE[26]), the two phase liquid method[27] and the isothermal vapor-phase epitaxy method (VPE[28]). The as grown crystals[29] of MMT and MCT are often p-type due to Hg vacancies. By annealing[30] the samples for a certain time in Hg vapor at low temperature they can be converted to n type. Delves[31] in 1965 started the work on semimagnetic semiconducting single crystals which Holm[23] and Furdyna and Leibler[32] et al. continued. Much of this research as well as work of more recent vintage, has been reviewed by Furdyna[33,34]. A thorough review of MMT with more than 150 references has been given by Rogalski[2].

Because MMT is paramagnetic, has the ZnS structure for all compositions at least up to $x \cong 0.35$, and because of many other similarities, Johnson[29] et al. assumed that in the absence of an applied magnetic field the physical properties of MMT for $x < 0.35$ are similar to those of MCT. This assumption was made based on the work of Furdyna[30] who mentioned in his paper that mobilities of $\mu \approx 10^5$ cm2/V.s or more were observed at 77K. However, there have not yet been electron mobility calculations for MMT which could be compared to MCT. The purpose of this paper is to collect the required band and material parameters and do the mobility calculations. Most of the parameters are obtained from experiment. They will be combined with a calculational model already used for MCT and MZT, transport properties of MMT in the absence of a magnetic field will be obtained, and the results will be compared with those of MCT for the same energy gap.

Since the band structure of MMT in the absence of a magnetic field does not show any effects caused by the magnetic ions it can be described by Kane's theory[35,36]. Under this condition the procedure of calculating the electron mobility in n-type MMT and the concentration of the free carriers would be the same as in our previous calculations of MZT[3,4,37].

An outline of the model used is given in section II, values of the band and material parameters extracted from experiments are given in section III, calculations and results are given in section IV and finally conclusions are given in section V.

II Theory:

As was mentioned before the wave functions of the conduction electrons and the dispersion relation are described by the Kane three band model[3] in the absence of a magnetic field. The non-parabolicity of the energy band has been considered. Due to the high ionicity of the material and the importance of the optical phonon interaction, the relaxation time approximation could not be used and a numerical technique has to be used in solving the Boltzman equation. In setting up the Boltzmann equation, the interaction of the electrons with the ionized impurities, heavy holes, alloy disorder, acoustic phonons and polar optical phonons were considered. At low temperature the scattering is mainly due to ionized impurities. The charged impurity atoms do not scatter high energy electrons and this scattering process decreases with increasing temperature. Optical phonon scattering is predominant at high temperature and the Frolich perturbation potential is used to describe the interaction. For acoustic phonons, the deformation potential which arises from the changes in the energy band gap as a result of the changes in the spacing of the lattice atoms is used. In mixed alloys, like MMT, Hg and Mn are randomly distributed in the crystal. Since a virtual crystal is assumed for band structure purposes, the disorder in the crystal is taken care of by the scattering of electrons from the alloy disorder. The details of the calculations of each scattering mechanism, the model used for the donor levels, the neutrality equation and the variational principles technique used in solving the Boltzmann equation are given in (3, 37, 38-42). Screening effects are included in the interaction with ionized impurities, holes and optical phonons.

Since MMT contains the magnetic ions Mn^{++}, the total electronic Hamiltonian[30] is given by

$$H = H_0 + H_{ex} = H_0 + \sum_{R_i} J(r - R_i) S_i \cdot \sigma, \qquad (1)$$

where H_0 is the Hamiltonian term for a nonmagnetic semiconductor, H_{ex} is

the term which takes care of the exchange interaction of the band electrons with the localized magnetic moments, S_i and σ are the spin operators of Mn++ and of the band electron, respectively, J is the electron-ion exchange coupling constant, and r and R_i are the band electron and Mn++ coordinates, respectively. The summation is taken over all the lattice sites occupied by Mn++ ions. Furdyna[30] pointed out that since the electronic wave function is very extended, the electron encounters many Mn++ ions at any time and S_i could be replaced by the thermal average $< \vec{S} >$ of the Mn++ spin of all ions. For a magnetic field in the z direction and in the paramagnetic phase $< \vec{S} >$ can be replaced be $< S_z > \hat{k}$. Thus, also using the virtual crystal approximation,

$$H_{ex} = \sigma_z < S_z > x \sum_{\vec{R}} J(\vec{r} - \vec{R}), \qquad (2)$$

where the sum now runs over all sites. $< S_z >$ is proportional to the magnetization which vanishes in the absence of an external field for a paramagnet. It is then clear from equation (2) that the exchange term will also vanish in the absence of a magnetic field, at least in the paramagnetic phase. MMT is paramagentic[30] at the composition and temperature we are interested in.

III. Parameters for electron mobility and charge carrier concentration calculation for $Hg_{1-x}Mn_xTe$:

Mercury telluride crystallizes in the zinc blende type structure with a lattice constant a = 6.461A°, while manganese telluride crystallizes in the hexagonal NiAs type structure with lattice constants[43] a = 4.15 A° and c = 6.71 A° . X-ray measurements and differential thermal analysis were performed by Delves and Lewis[44] for the HgTe-MnTe system and the following three phases were observed in the solid solution: (1) α phase with the zinc blende type structure $(0 \leq x \leq 0.36)$, (2) α phase plus $MnTe_2$ with the pyrite structure $(0.36 \leq x \leq 0.75)$, and (3) MnTe with NiAs type structure (x > 0.75). For $x < 0.36$, $Hg_{1-x}Mn_xTe$ crystal growth behaviour is very similar to that of $Hg_{1-x}Cd_xTe$ for comparable[2] x . For $x > 0.36$, $Hg_{1-x}Mn_xTe$ has more than one crystallographic phase which makes the material not favorable for devices applications.

The energy gap in MMT behaves in the same manner as in the MCT. It changes from a negative band gap semimetal to a positive band gap semiconductor as the composition x, (which gives the concentration of Mn

in MMT or Cd in MCT), increases from zero. A zero band gap is achieved at 4.2K temperature[29], when x=0.07 in MMT and when x=0.15 for MCT. The change in MMT energy gap with x is twice as fast as it is in MCT[30]. The equation deduced from experiments for the energy gap ($\Gamma_6 - \Gamma_8$) as a function of those two terms has been given by Kaniewksi and Mycielski[45],

$$E_g(x, T) = -0.253 + 3.446x + 4.9 * 10^{-4}T - 2.55 * 10^{-3}xT \quad (eV).$$

The Kane momentum matrix element was obtained from interband magnetooptics experiments [46,47] and it is a function of the composition[48] x, $P(x) = (8.35 - 7.94x) \times 10^{-8} eVcm$.

Gebicki and Nazarewicz[49] measured the infrared reflection spectra in the optical region from 50 to 300 cm^{-1} at 90 and 295 K of MMT with $0 \le x \le 0.69$. These crystals were grown by the Bridgman method and their crystallographic structure was tested by X-ray diffraction to ensure they have the zincblende structure. They obtained the dielectric functions versus wave number by applying the Kramers-Kronig analysis to the reflection spectra. The position of the maxima of $\mathrm{Im}\varepsilon(\omega)$ and $\mathrm{Im}(-1/\varepsilon(\omega))$ indicate the long-wavelength phonon frequencies for transverse and longitudinal optical phonons respectively. For each value of x, two frequencies of the transverse optical phonons and two of the longitudinal optical phonons were found as is consistent with "two-mode" behaviour" of the phonon spectra. They calculated the long-wavelength optical phonon frequencies as a function of composition using the random-element isodisplacement (REI) model [50,51] which is applicable only for the composition range at which the crystal structure does not change. For this reason the unknown parameters of the REI model were determined from the optical phonon frequencies for x = 0 (HgTe) and x = 0.69. The x = 1 (MnTe) data cannot be used because the change of the crystal structure causes discontinuity of the phonon spectra. When they compared their theoretical results for the composition range $0 \le x \le 0.69$ with experiment they obtained good agreement. Using their results for the dependence of long-wavelength optical phonon frequencies on composition we extracted the frequency equations we needed for our model using linear interpolation between the points x = 0 and x ≅ 0.4 (where the curve was linear). We obtained:

$$\omega_{LO}(HgTe) = 134 - 5x, \qquad \omega_{TO}(HgTe) = 110 + 27.5x$$
$$\omega_{LO}(MnTe) = 187 + 25x, \qquad \omega_{TO}(MnTe) = 187 - 5x$$

The Callen effective charge, e_c^*, which is related to the relative displacements of atoms in a unit cell, determines the strength of the interaction of the electrons with the LO-phonon (see reference 39, page 80). The Szigeti effective charge, e_S^*, and the total transverse charge are related to the Callen effective charge by the relations:

$$e_c^* = \left[\frac{\varepsilon_\infty + 2}{3\varepsilon_\infty}\right] e_S^* \qquad \text{and} \qquad e_c^* = \frac{e_T^*}{\varepsilon_\infty}$$

In reference (51), Gorska et al. made the assumption that the charges e_B and e_c in the REI theoretical model are the Szigeti effective charges

$$e_B = e_{AB}^*, \qquad e_c = e_{AC}^*.$$

W. Gbicki et al.[49], in their calculation of optical phonons in MMT took the effective charge of all ions to be equal to that of HgTe[42]

$$e_A/e = e_B/e = e_c/e = 0.6$$

Using these equations and the values mentioned earlier for the dielectric constants for HgTe and MnTe, the transverse charges are:

$$e_T^*(HgTe) = 3.44, \quad e_T^*(MnTe) = 3.32.$$

The parameters needed for the interaction of the electrons with the acoustic phonons are the longitudinal and transverse sound velocities and the deformation potentials[42]. The longitudinal and transverse acoustic waves has the simple relations[52], $v_l = \sqrt{\frac{c_{11}}{\rho}}$ and $v_t = \sqrt{\frac{c_{44}}{\rho}}$. Because of the lack of measurements done on MnTe and due to the fact that the Mn portion is very small, we assume the Mn causes a negligible change in v_l and v_t. Using the longitudinal and transverse sound velocities[52] of HgTe, $c_{11} = 5.361 \times 10^{11}$ dyne/cm^2, $c_{44} = 2.123$ dyne/cm^2 and the density [2] of HgTe = 8.076 (gm/cm^3), the longitudinal and transverse velocities can easily be estimated. We obtain $v_l = 2.576 \times 10^5$ cm/sec and $v_t = 1.621 \times 10^5$ cm/sec.

For MMT a virtual crystal was assumed and the band structure was described by the Kane theory. The compositional disorder is considered in the scattering of the electrons. It is treated as a random distribution of square-well scattering centers with dimensions of a unit cell and with a depth approximately equal to the difference between the band gaps of the end-point compounds[38]. Using the Energy gap[2] values at 4.2K^0 of HgTe and MnTe when they both have the zinc blende structure we got a value of

3.5eV for the disorder energy (E_{dis}). These results as well as values for all other needed quantities are summarized in Table (1).

IV. Calculations and Results:

MCT and MMT are compared for two different values of MMT enrgy gap. The first value of MMT energy gap, x (MMT) = 0.0923, is chosen to give values of the MMT energy gap that are very close to those of MCT, with x(MCT) = 0.193, at low temperature (see fig. 1). This value was chosen as typical for energy gaps appropriate to the 10 μm window. Other appropriate values of x can be used with equal facility in our mobility calculations. The second value of MMT energy gap, x(MMT) = 0.094, is chosen to give values of the MMT energy gap that agrees with those of MCT with x = 0.193 at intermediate temperature (see fig. 3). In both cases we used a donor concentration equal to $N_d = 3 \times 10^{14}$ /cm^3 and acceptor concentration equal to $N_a = 0$. In each case we considered two kinds of donors, one kind is ionized with an energy which merges with the conduction band and a concentration chosen so that $N_d - N_a$ is equal to the concentration of electrons in MCT at very low temperature[40]. The second kind are bound donors with a concentration and ionization energy chosen to fit the concentration of the electrons vs temperature at low temperature for MCT[40]. For the concentrations considered, the second donor had very little effect. When the electron mobility in both cases were calculated and compared they came out to be very close (see graphs 2 and 4) at high temperatures but differed by about 30% at liquid nitrogen temperatures. When another value of the MMT disorder energy, 1.8eV, was used the mobility value was increased by approximately 25% over the whole range of temperature.

V. Conclusions

Since MMT shares the same electronic properties as MCT for the same energy gap and since it has the advantages that were mentioned earlier, it is another strong candidate for use in infrared detectors. However, Brimrose apparently continues to be the only company which makes MMT detectors commercially. The possibility of varying the electronic properties of MMT by use of a magnetic field makes MMT a very intertesting material. The effects of this on the mobility await further study.

References

* Research supported by NASA/Marshall Space Flight Center, Grant No. NAG8-781, Supplement 2.

1) W. E. Spicer, J. A. Silberman, I. Lindau, A. B. Chen, A. Sher and J. A. Wilson, J. Vac. Sci. Technol. A1, 1735 (1983).
2) Antoni Rogalski, Infrared Phys., 31, No. 2, pp. 117-166 (1991).
3) Wafaa Abdelhakiem Gobba, "Theory of electron mobility in narrow-gap semiconductors", Ph. D thesis, Florida Institute of Technology, (1991).
4) Wafaa Abdelhakiem, J. D. Patterson and S. L. Lehoczky, Materials letters 11(12), 47-51 (1991).
5) A. Sher, A. B. Chen, W. E. Spicer and C. K. Shih, J. Vacuum Sci. Technol. A3 , 105 (1985).
6) W. A. Harrison, J. Vacuum Sci. Technol. A1, 1672 (1983).
7) A. B. Chen, A. Sher and W. E. Spicer, J. Vacuum Sci. Technol. A1,1674 (1983).
8) N. P. Gavaleschko, P. N. Gorlei and V. A. Schendirovski, Uzkozonnye poluprovodniki. Poluchenie i Fizicheskije Svojstva. Naukova Dumka, Kiev (1984).
9) R. Tirboulet, M. Bourdillot, A. Durand and T. Nguyen Duy, Proc. SPIE 1106, 40 (1989).
10) K. C. Hass and H. Ehrenreich, J. Crystal growth 86, 8 (1988).
11) P. Becla, P. A. Wolff, R. L. Aggarwal and S. Y. Yuen, J. Vac. Sci. Technol. A3, 116 (1985).
12) R. R. Galazka, J. Cryst. Growth 72, 364 (1985).
13) S. Wong and P. Becla, J. Vac. Sci. Technol. A4, 2019 (1986).
14) A. Wall, C. Caprile, A. Franciosi, R. Reifenberger and U. Debska, J. Vac. Sci. Technol. A4, 818 (1986).
15) V. I. Kalenik, I. N. Gorbatiuk, I. M. Rarenko, O. A. Bodnaruk, O. D. Pustylnik, S. E. Ostapov, V. P. Schafraniuk and A. F. Slonecki, in Impurity and Defects of Narrow Gap semiconductors, Proc. 2nd AU-Union Symp. Povlodar, Part 1, p. 87 (1989) (in Russian).
16) Infrared Products Brimrose Corporation, 5020 Campbell Blvd, Baltimore, MD p. I-4. A brochure from this company.
17) R. R. Galazka, in Proceedings of the 14th International Conference on the Conductors, Edinburgh, 1978, edited by B. L. H. Wilson (IOP, London, 1978), p. 133.
18) R. R. Galazka and J. Kossut, in Narrow Gap semiconductors: Physics

and Applications, Vol. 133 of Lecture Notes in Physics, edited by W. Zawadki (Springer, Berlin, 1980), p. 245.

19) J. A. Gaj, in Proceedings of the 15th International Conference on the Physics of Semiconductors, Kyoto, 1980 [J. Phys. Soc. Jpn. Suppl. A49, 747 (1980)].

20) T. Dietl, Physics in High Magnetic Field, Vol. 24 of Springer Series on Solid State Sciences, edited by S. Chikazumi and N. Miura (Springer, Berlin, 1981), p. 344.

21) J. K. Furdyna, J. Appl. Phys.53, 7637 (1982).

22) R. T. Delves, Br. J. Appl. Phys. 16, 343 (1965).

23) R. T. Holm and J. K. Furdyna, Phys. Rev. B15, 844 (1977).

24) P. Becla, D. Heiman, J. Misiewicz, P. A. Wolff and D. Kaiser, SPIE 796, 108 (1987).

25) R. Triboulet, D. Triboulet and G. Didier, J. Crystal Growth 38, 82 (1977).

26) U. Debska, M. Dietl, G. Grabecki, E. Janik, E. Kierzek-Pecold and M. Klimkiewicz, Physica Status Solidi 64a, 707 (1981).

27) I. E. Lopatynski, Inorg. Mater. 12, 296 (1976).

28) P. Becla, J. Lagowski, H. C. Gatos and L. Jedral, J. Electrochem. Soc. 129, 2855 (1982).

29) W. B. Johnson and J. R. Anderson, Phys. Rev. B 29(12), 6679(1984).

30) J. K. Furdyna, J. Vac. Sci. Technol., 21(1), 220 (1982).

31) R. T. Delves, Br. J. Appl. Phys. 16, 343 (1965).

32) K. Leibler, W. Giriat, Z. Wilamowski, and R. Iwanowski, Phys. Status Solidi B47, 405 (1971).

33) J. K. Furdyna, J. appl. Phys. 64, R29 (1988).

34) R. K. Willardson and A. C. Beer (Treatise Eds), Semiconductors and Semimetals, Vol. 25 (Volume edited by J. K. Furdyna and J. Kossut). Academic, Boston (1988).

35) M. Jaczynski, J. Kossut, and R.R. Galazka, phys. stat. sol. (b) 88, 73 (1978).

36) Evan O. Kane, J. Phys. Chem. Solids 1, 249-261 (1957).

37) J.D. Patterson, Wafaa A. Gobba and S.L. Lehoczky,"Electron mobility in n-type $Hg_{1-x}Cd_xTe$ and $Hg_{1-x}Zn_xTe$ allos", J. of Materials Research, to be published, August 1992.

38) D. A. Nelson, J. G. Broerman, C. J. Summers, and C. R. Whitset, Phys. Rev. B18 (4), 1658-1672 (1978).

39) S. L. Lehoczky, F. R. Szofran, and B. G. Martin, NASA CR-161598, "Advanced Methods for preparation and Charactrization of Infrared Detector Materials, Part I", July 5, 1980.

40) S. L. Lehoczky, C. J. Summers, F. R. Szofran, and B. G. Martin, in Materials Processing in the reduced Gravity Environment of Space, Guy E. Rindone, Ed., Elsevier, Amsterdam, 1982, pp. 421-431.
41) S. L. Lehoczky, F. R. Szofran, in Materials Processing in the Reduced Gravity Environment of Space, Guy E. Rindone, Ed., Elsevier, Amsterdam, 1982, pp. 409-420.
42) S. L. Lehoczky, J. G. Broerman, Donald A. Nelson, and Charles R. Whitset, Phys. Rev. B9, 1598-1620 (1974).
43) W. Giriat and J. K. Furdyna, Semiconductors and Semimetals, Vol. 25 (Edited by R. K. Willardson and A. C. Beer), p.1. Academic, Boston (1988).
44) R. T. Delves and B. Lewis, J. Phys. Chem. Solids 24, 549 (1963).
45) J. Kaniewski and A. Mycielski, Solid St. Commun. 41, 959 (1982).
46) E. Janik and G. Karczewski, J. Electron. Mat. 16, 381 (1987).
47) G. Bastard, C. Rigaux, Y. Guldner, A. Mycielski, J. K. Furdyna and D. P. Mullin, Phy. Rev. B24, 1961 (1981).
48) R. R. Galazka and J. Kossut, Londolt-Börnstein, New Series 17b, (Edited by O. Madelung, M. Schulz and M. Weiss), p. 302. Springer, Berlin (1982).
49) W. Gebicki and W. Nazarewicz, Phys. Stat. Sol. (b) 80, 307 (1977).
50) H. Harada and S. Narita, J. Phys. Soc. Japan 30, 1628 (1971).
51) M. Gorska and W. Nazarewicz, Phys. Stat. Sol. (b) 65, 193 (1974).
52) Karl W. Boer, Survey of Semiconductor Physics: Electrons and other particles in bulksemiconductors, Van Nostrand Reinhold, p. 79-83.
53) D.L.Rode, Phys. Rev. B2, 4036 (1970).
54) A. Jedrzejczak and Dietl, Phys. Stat. Sol. 76b, 737 (1976).

Table 1

Parameters for electron mobility and charge carrier concentration calculations for $Hg_{1-x}Mn_xTe$

Parameter	value	reference
Lattice constant	$a(x) = 6.461 - 0.121x\ A^0$ $(0.08 \le x \le 0.30)$	(2)
spin-orbit splitting	$\Delta(eV) = 1.08$ $(0.08 \le x \le 0.30)$	(2)
$\Gamma_6 - \Gamma_8$ energy gap	$E_g(x,T) = -0.253 + 3.446x + 4.9 \times 10^{-4}T - 2.55 \times 10^{-3}xT \quad (eV)$ $(0.08 \le x \le 0.30)$	(45)
heavy hole effective mass	$m^*_{hh}/m_0 = 0.5$	(2)
momentum matrix element coupling conduction and valence bands	$P(x) = (8.35 - 7.94x) \times 10^{-8} eVcm$	(48)
static dielectric constant	$\varepsilon_0 = 20.5 - 32.6x + 25.1x^2$	(2)
high frequency dielectric constant	$\varepsilon_\infty = 15.2 - 28.8x + 28.2x^2$	(2)
HgTe LO phonon frequency	$\omega_{LO}(HgTe) = 134 - 5x$ cm-1	(49)
HgTe TO phonon frequency	$\omega_{TO}(HgTe) = 110 + 27.5x$ cm-1	(49)
MnTe LO phonon frequency	$\omega_{LO}(MnTe) = 187 + 25x$ cm-1	(49)
MnTe TO phonon frequency	$\omega_{TO}(MnTe) = 187 - 5x$ cm-1	(49)
transverse effective charges	HgTe $e_T/e = 3.44$	(39,42,49,51)
	MnTe $e_T/e = 3.32$	
deformation potentials(23)	$E_0 = 9.5$ eV longitudinal mode	(53)
	$E_1^{(a)} = 4$ eV transverse mode	(42)
	$E_2 = 3$ eV transverse mode	(54)
longitudinal sound velocity	$v_l = 2.576 \times 10^5$ cm/sec	(52)
transverse sound velocity	$v_t = 1.621 \times 10^5$ cm/sec	(52)
Hg mass	$m_{Hg} = 200.59$ a.m.u.	
Mn mass	$m_{Mn} = 54.938$ a.m.u.	
Te mass	$m_{Te} = 127.60$ a.m.u	
reduced mass	$m_{HgTe} = 1.295 \times 10^{-22}$ g	

	$m_{MnTe} = 0.615 \times 10^{-22}g$	
disorder energy	$E_{dis} = 3.5eV$	(2),(38)

---

a) using hydrogenic approximation

List of Figures

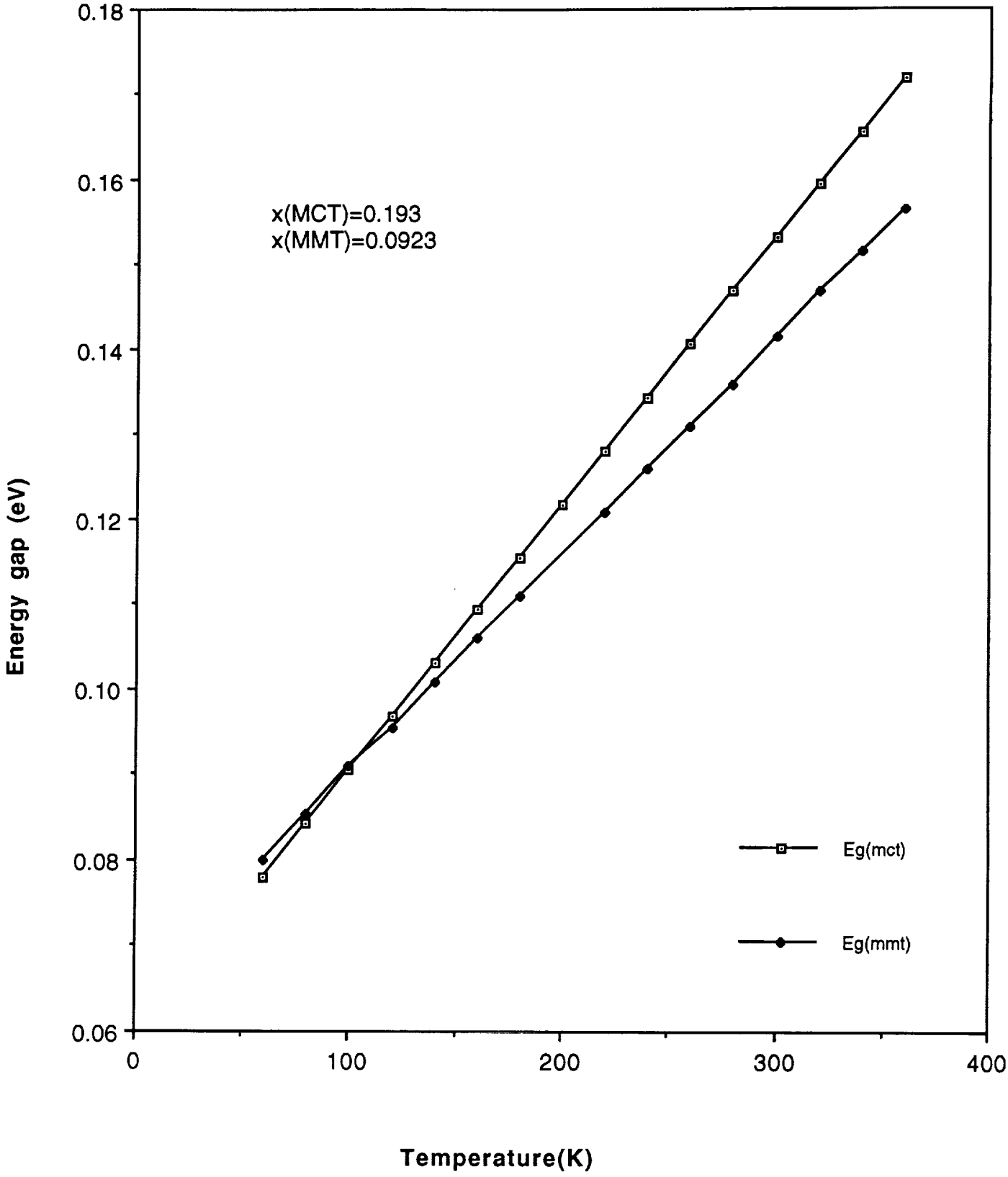

Fig. 1. A comparison between MCT and MMT energy gap vs. temperature.

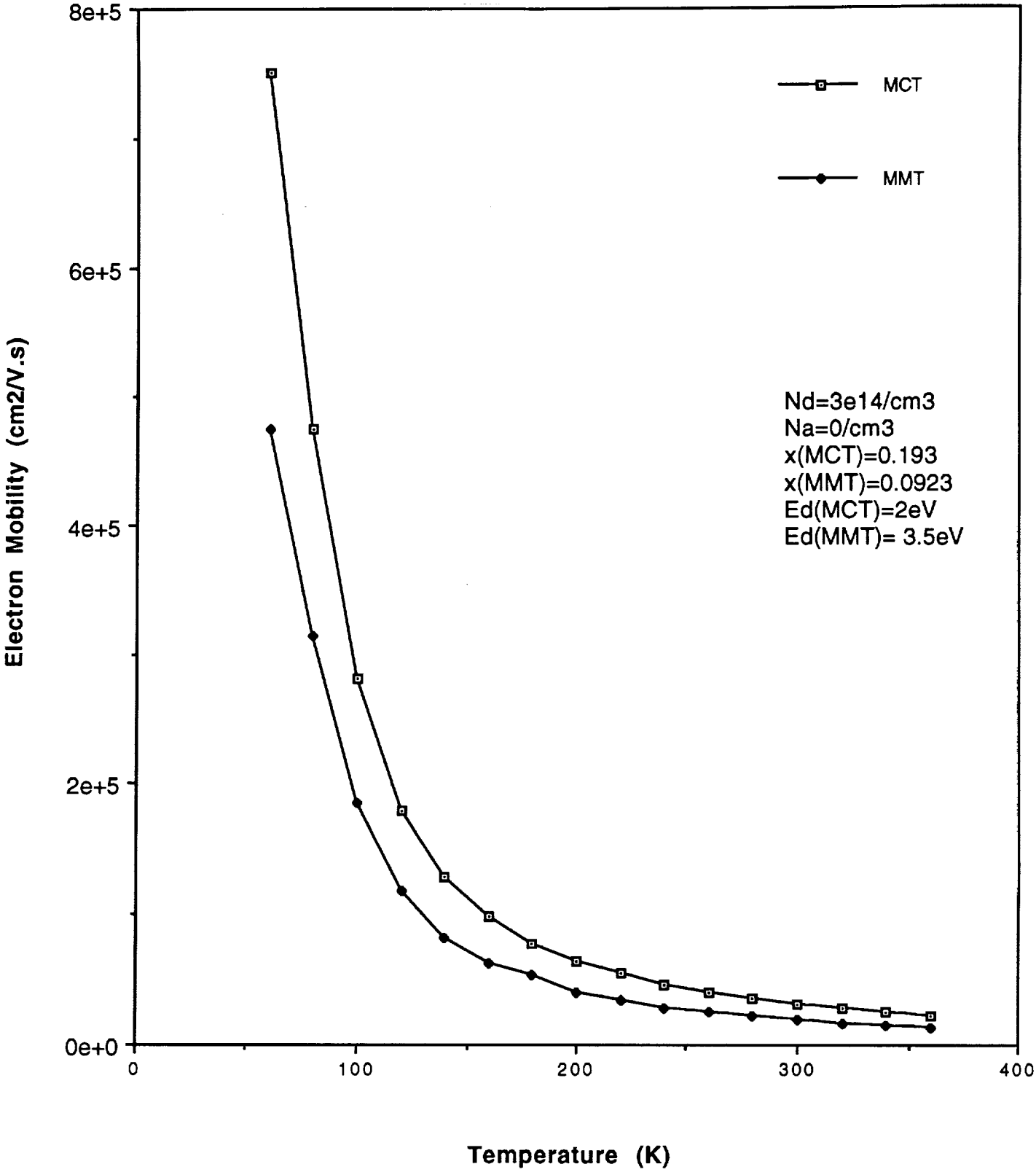

Fig. 2. A comparison between MCT and MMT electron mobility vs. temperature

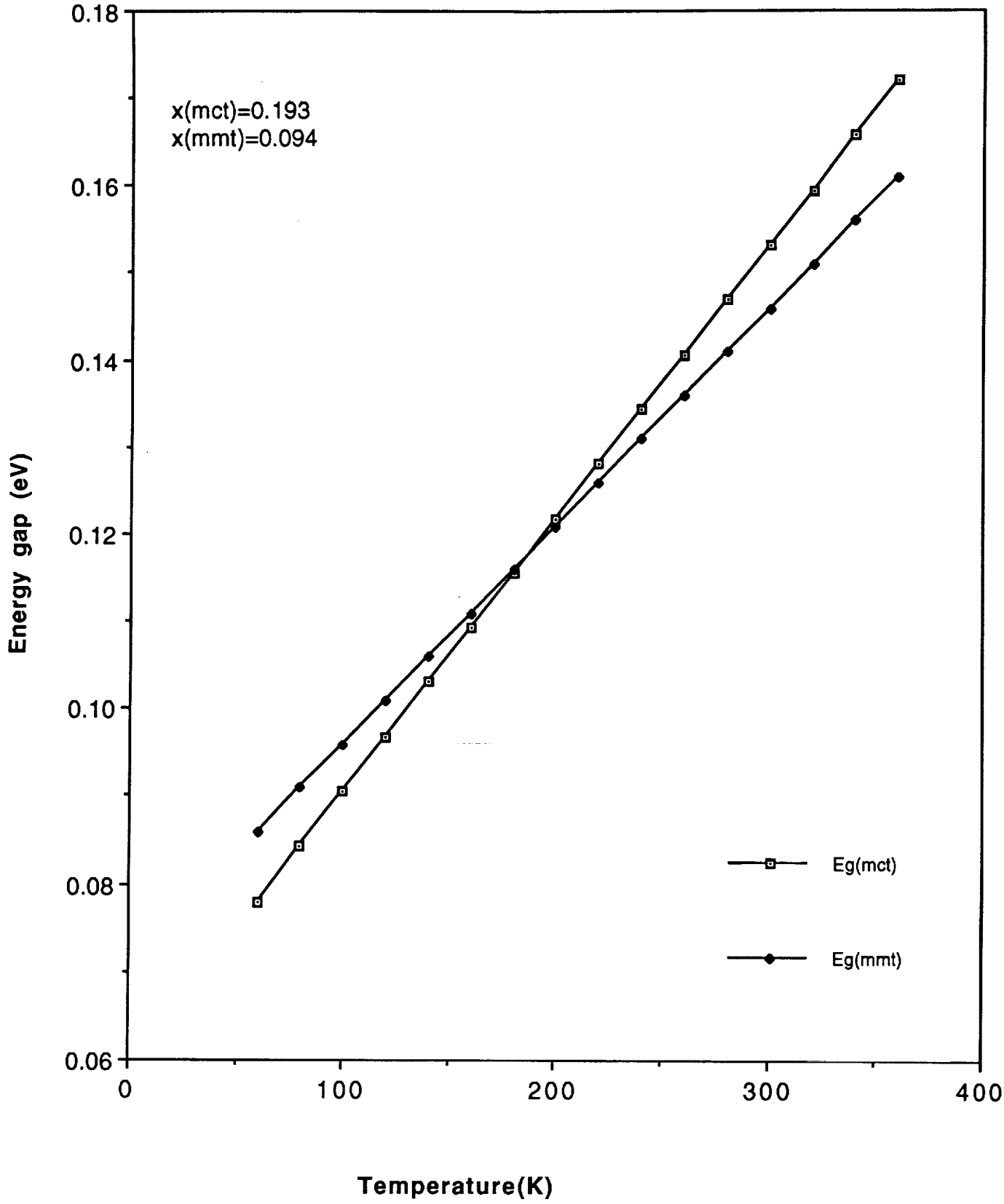

Fig. 3. A Comparison betwee MCT and MMT energy gap vs. temperature.

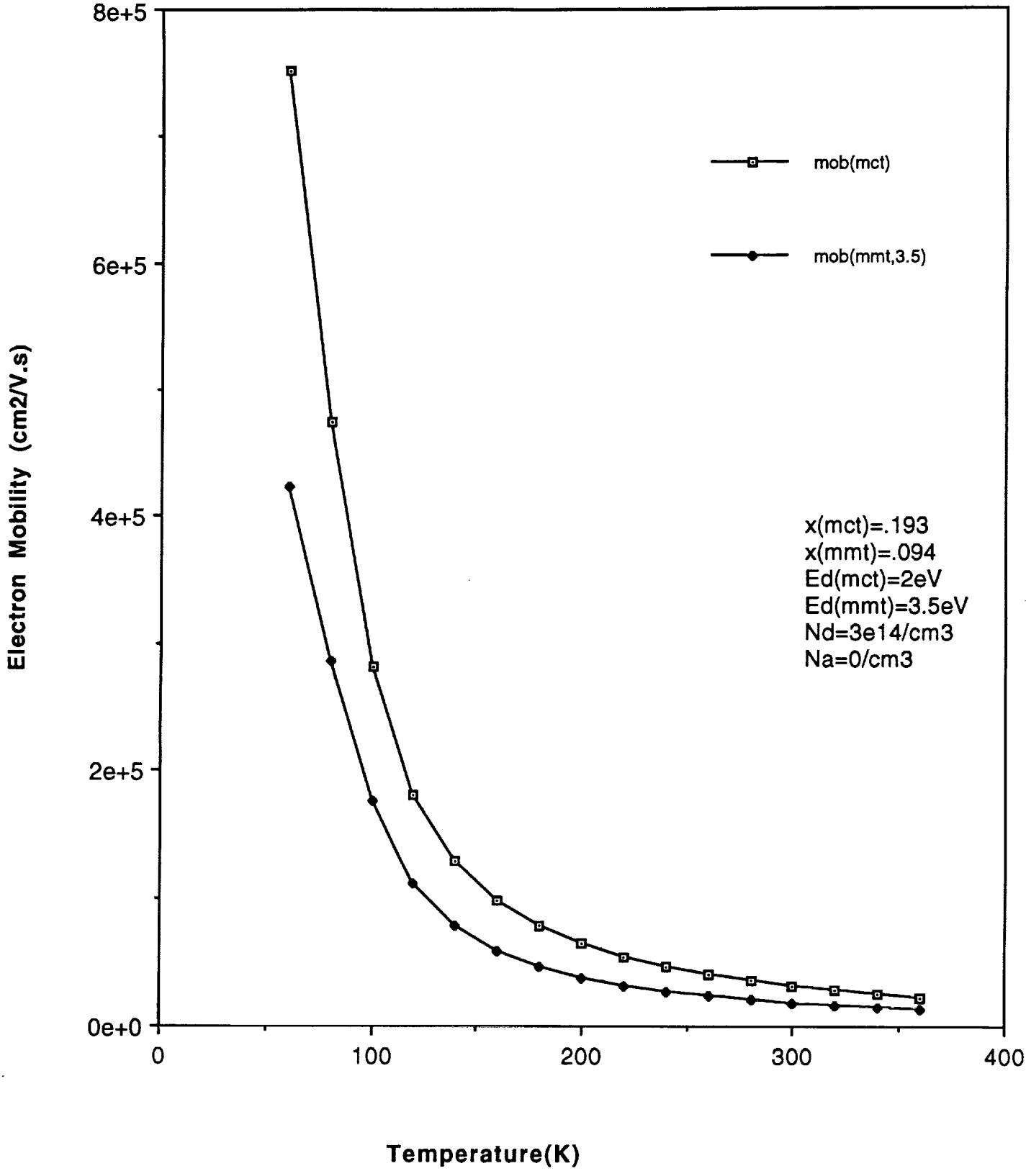

Fig. 4. A Comparison between MCT and MMT electron mobility vs. temperature.

I. References

We have given above a few particularly relevant references for each topic. An extensive list of references has been computerized by us. We have listed it by topics in the appendix.

J. Availability of Program

We have the program written in Fortran, and stored on a Sun, a Vax and a Nighthawk. However, because we have local networks as well as Internet, we can move the program around easily from computer to computer (on campus, in state or even out of state). Thus we could send our program or results to a properly networked terminal at Marshall Space Flight Center. The programs for MCT, MZT and MMT are also available on disks that are available as required.

II. LIST OF REPORTS AND DOCUMENTS

1. James D. Patterson, Further Improvements in Program to Calculate Electronic Properties of Narrow Band Gap Materials, Semi-Annual Report, NAG8-781 Supplement 2, December 15, 1991.

2. Wafaa M.K.A. Gobba, "Theory of Electron Mobility in Narrow Gap Semiconductors," Ph.D. Thesis, Florida Institute of Technology, August 1991.

3. J.D. Patterson, Wafaa A. Gobba, and S.L. Lehoczky, "Electron Mobility in n-type HgCdTe and HgZnTe Alloys," To be published in the Journal of Materials Science.

4. J.D. Patterson and Wafaa A. Gobba, "The Physics of Astronomical Infrared Detectors," I.A.P.P.P. Communications 47, 1-16 (1992).

5. Wafaa A. Gobba, "Theoretical Calculations of Electron Mobility in Narrow-Gap Semiconductors," AAPT Announcer 21, 54-55 (!991). Invited talk presented at January 1992 Orlando Meeting of Am. Assoc. of Phys. Teachers.

6. Wafaa A. Gobba, J.D. Patterson, and S.L. Lehoczky, "Electron Mobility in Mercury Zinc Telluride Alloys," Bull. Am. Phys. Soc. 37(1), 73 (1992).

7. J.D. Patterson and Wafaa A. Gobba, "Enhanced Screening in Doped Semiconductors," Bull. Am. Phys. Soc. 37(1), 196 (1992).

8. Previous reports and papers were listed in Final Report for NAG8-781 (June 15, 1991). These include Wafaa Abdelhakiem, J.D. Patterson, and S.L. Lehoczky, "A Comparison between electron mobility in n-type $Hg_{1-x}Cd_xTe$ and $Hg_{1-x}Zn_xTe$, Materials Letters 11, 47-51 (1991).

9. Wafaa A. Gobba, "Theoretical Calculations of Electron Mobility and Charge Carrier Concentration in Mercury Zinc Selenide," proposal to NRC, April 1992.

III. ABSTRACTS OF PAPERS, REPORTS AND OTHER DOCUMENTS

SEMI-ANNUAL REPORT

TITLE OF GRANT

Further Improvements in Program to Calculate Electronic Properties of Narrow Band Gap Materials

TYPE OF REPORT

Brief Summary of Project

NAME OF PRINCIPAL INVESTIGATOR

James D. Patterson

PERIOD COVERED BY THE REPORT

June 15, 1991 - December 15, 1991

NAME AND ADDRESS OF GRANTEE INSTITUTION

Florida Institute of Technology
150 W. University Boulevard
Melbourne, FL 32901

GRANT NUMBER

NAG8-781 Supplement 2
George C. Marshall Space Flight Center
Marshall Space Flight Center, AL 35812
(Technical Officer Sandor L. Lehoczky, ES75)

Theory of electron mobility in narrow-gap semiconductors

by

Wafaa M.K. Abdelhakiem Gobba
B.S. in Physics, Cairo University, 1977
M.S. in Physics, Florida Institute of Technology, 1984

A Dissertation submitted to the department of Physics and Space Sciences and the Graduate School of Florida Institute of Technology in partial fulfillment of the requirement for the degree of Doctor of Philosophy.

Under the supervision of Professor James D. Patterson

Florida Institute of Technology
Melbourne, Florida
August 1991

ABSTRACT

The electron mobility, concentration of electrons, light holes and heavy holes, and Fermi energy in n-type $Hg_{1-x}Zn_xTe$ (MZT) have been calculated and compared with those of $Hg_{1-x}Cd_xTe$ (MCT) for the same energy gap (but different x), and the same donor and acceptor concentration. The results for MZT were found to be very close to those of MCT. The calculation relied on solving the Boltzmann transport equation using variational principals. The processes that were of significance included the scattering of electrons by: ionized impurities, holes, compositional disorder, acoustical phonons and optical phonons. In the process of calculating the results for MZT a table for the latest values of all the needed material parameters was obtained by a literature search.

MZT has been considered as a substitute for MCT for possible use in infrared detectors due to its relative stability and hardness. Our theoretical results for MZT were compared to the experimental results published by Rolland et al. and Granger et al. and very good agreement over most of the temperature range was obtained.

The effect of making changes on some of the relevant parameters in the calculation was checked. Also, adding neutral impurities to the scattering processes and using the most recent published band parameters of MCT (rather than the slightly older values) on the electron calculation did not produce significant changes.

The speed of a very involved and long program has been increased by changing its code from Basic for an HP 9845 to FORTRAN for a Vax 11/780 and later a Sun workstation 386i. This program was given to us by Dr. S.L. Lehoczky and it was written to calculate the electron mobility, the free carrier concentrations, and the Fermi energy for MCT. All of these were calculated as a function of temperature, composition, donor, and acceptor concentration. The program was checked, corrected and fine tuned by including the latest values of material parameters for MCT, another version was made to fun for MZT and neutral defect scattering was added to the program.